



NTNU – Trondheim
Norwegian University of
Science and Technology

Modeling of Aquaculture PET Net with the Use of Finite Element Method

Claudia Casanova
Widyasatka Dwikartika

Marine Coastal Development

Submission date: June 2013

Supervisor: Harald Ellingsen, IMT

Co-supervisor: Østen Jensen, SINTEF Fisheries and Aquaculture

Norwegian University of Science and Technology
Department of Marine Technology

TMR 4905 – Master Thesis Marine Systems - spring 2013

Student: Claudia Casanova and Widyasatka Dwikartika

Modeling of Aquaculture PET Net with the Use of the Finite Element Method

Background:

Since the increase in demand for fish, aquaculture has been expanding rapidly. In many countries the coastal aquaculture is faced with strong resistance from other industries and therefore the aquaculture industry has to move into more open waters. Moving into more exposed areas require alternative technology and material for the design of the fish cages. Therefore, recently there have been many studies with regard to different materials used for nets. Due to complexity of the net-cage system it is not always easy to study the behavior of the net cage system analytically. In most cases complicated numerical simulations need to be developed and verified through experiments. However, some net materials such as PET are a very stiff material and have limited deformation capacity compared to the commonly used nylon net. Therefore, it is hypothesized that deformation of stiff net like PET can be predicted by simple structural analysis, instead of using complicated hydrodynamic models.

SINTEF Fisheries and Aquaculture conducted several experiments of net panels with different bending stiffness. The experiments include the effects of flow speed and angle of attack, the deformation of nets normal to uniform currents and the oscillation of net panel. All the experiments were conducted in the North Sea Center flume tank in Denmark. The results of these experiments have been used as basis for comparisons with the theoretical analyses performed in this work.

Objective:

The objectives of this master study are to:

- Construct the PET net panel model in ABAQUS corresponding to the net specifications in SINTEF experiment.
- Analyze the bending of the net panel at various loads that corresponds to different current velocities in the experiment.
- Comparison of the result between ABAQUS and SINTEF experiment to determine if simple structural analysis can predict the bending or deformation of the net panel.

Scope of Work:

In this master thesis the candidates shall perform the following main activities:

1. Develop a structural modeling of a Polyethylene Terephthalate (PET) net panel by using finite element software (ABAQUS). The model shall be built corresponding to the net panel experiments performed by SINTEF Fisheries and Aquaculture.
2. Simulate the current forces from the experiments by using line loads completely distributed over the net panel model.

3. Compare the theoretical results with the experiment and discuss and explain possible deviations.

General

The work shall be carried out and reported in accordance with guidelines, rules and regulations pertaining to the completion of a Master Thesis in engineering at NTNU.

The work shall be completed and delivered electronic by: June 10th, 2013.

Main advisor is Professor Harald Ellingsen, Department of Marin Technology, NTNU
Co-advisor is research director Arne Fredheim, SINTEF Fisheries and Aquaculture.

Trondheim, February 27th, 2013



Harald Ellingsen

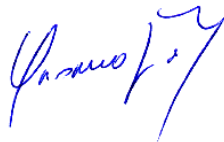
ACKNOWLEDGEMENTS

This master thesis has been finished as an accomplishment of two years master study in *Marine Coastal Development Program* at Norwegian University of Science and Technology (NTNU). The topic of this master thesis was given by SINTEF Fisheries and Aquaculture.

We are grateful to Prof. Harald Ellingsen as our supervisor for introducing us to the Aquaculture topic as well as for the support during our master thesis work. We would like also to thank Arne Fredheim as our co-supervisor who has guided us by given suggestions for which problems that should be pursued during this project.

The guidance and support received from Lars Gansel, Østen Jensen, Martin Føre and Per Christian Endresen from SINTEF Fisheries and Aquaculture was vital for the success of this work. We are very grateful due to their contribution by providing data from the experiment and expend their time by having meetings and mail discussions.

Special thanks for PhD candidates Ekaterina Kim and Mohamed Shainee who have supported and helped us in putting pieces together.



Claudia Casanova



Widiasatka Dwikartika

Table of Contents

| | |
|---|------|
| ACKNOWLEDGEMENTS..... | iii |
| Table of Contents..... | iv |
| List of Figures..... | vi |
| List of Tables..... | viii |
| ABSTRACT..... | ix |
| INTRODUCTION..... | 1 |
| 1.1 Background..... | 1 |
| 1.2 Objectives..... | 1 |
| 1.3 Scope of Work..... | 2 |
| CHAPTER 2..... | 3 |
| NET MATERIAL..... | 3 |
| 2.1 Net Types..... | 3 |
| 2.2 Material Properties..... | 5 |
| Bending Stiffness..... | 6 |
| Stress definition..... | 7 |
| Strain definition..... | 9 |
| 2.3 Net Geometry..... | 11 |
| CHAPTER 3..... | 13 |
| FINITE ELEMENT METHOD..... | 13 |
| 3.1 Introduction..... | 13 |
| 3.2 Nodes, Elements, and Degree of Freedom..... | 15 |
| 3.3 Beam Element..... | 16 |
| Euler –Bernoulli beam element..... | 17 |
| Timoshenko Beam element..... | 18 |
| 3.4 Mesh..... | 20 |
| 3.5 Formula..... | 21 |
| 3.6 Static Analysis..... | 21 |
| 3.5 ABAQUS Software..... | 22 |
| Beam element..... | 24 |
| Beam element formula..... | 26 |
| CHAPTER 4..... | 28 |
| APPLIED FORCE..... | 28 |
| 4.1 Uniform Load..... | 28 |
| CHAPTER 5..... | 30 |
| SINTEF EXPERIMENT..... | 30 |
| 5.1 Description..... | 30 |
| 5.2 Experiment Data..... | 31 |
| 5.3 Result..... | 32 |
| CHAPTER 6..... | 34 |
| MODELING..... | 34 |
| 6.1 Methodology Overview..... | 34 |

| | |
|---|----|
| Part..... | 36 |
| Property | 36 |
| Mesh | 37 |
| Step | 38 |
| Load..... | 39 |
| Boundary conditions | 40 |
| CHAPTER 7 | 42 |
| MODELING RESULTS | 42 |
| 7.1 Validation of model..... | 42 |
| Forces | 42 |
| Strain vs. Stress | 42 |
| 7.2 Comparison with SINTEF Experiment | 43 |
| 7.3 Displacement | 48 |
| Translation | 48 |
| Rotation..... | 50 |
| CHAPTER 8 | 52 |
| DISCUSSION, CONCLUSION | 52 |
| 8.1 Discussion..... | 52 |
| Secondary discussions..... | 53 |
| 8.2 Conclusion..... | 56 |
| RECOMMENDATION FOR FUTURE WORK..... | 57 |
| REFERENCES | 58 |
| APPENDIX | 61 |
| Average displacement at position (case 3) | 61 |

List of Figures

| | |
|--|----|
| Figure 1 Types of aquaculture net: (a) steel net, (b) copper net, (c) PET net, (d) Flattened expanded copper-nickel, (e) Chain-link woven brass, (f) Welded silicon-bronze, (g) Woven silicon-bronze, (h) Nylon knotless square net, (i) Nylon015 (Tsukrov et al., 2011), (Gansel et al., 2012)..... | 4 |
| Figure 2 Structural behavior due to external loads (Jianqiao, 2008)..... | 6 |
| Figure 3 Definition of stress (Ashby and Jones, 2012)..... | 8 |
| Figure 4 Simple tension and compression (Ashby and Jones, 2012)..... | 8 |
| Figure 5 three-dimensional stress element subjected to a combination of stress (Steffen, 2012)..... | 9 |
| Figure 6 elastic bending of beams (Ashby and Jones, 2012)..... | 10 |
| Figure 7 Stress-strain curves (Steffen, 2012)..... | 11 |
| Figure 8 PET net geometry..... | 11 |
| Figure 9 FEM paths from the real structure to the computational model (Onate, 2009)..... | 14 |
| Figure 10 Structural models (Onate, 2009)..... | 15 |
| Figure 11 Cylindrical structure is subdivided into a series of node and elements (Steffen, 2012)..... | 16 |
| Figure 12 A one-dimensional model (2-nodes and one element) represent its displacement ($U_{x(n)}$ & $U_{x(n+1)}$) in x-direction (Steffen, 2012)..... | 16 |
| Figure 13 Beam element with its local coordinate system: physical coordinates x, natural coordinate ξ (Quek and Liu, 2003)..... | 17 |
| Figure 14 Beam under distributed load (Logan, 2012)..... | 18 |
| Figure 15 Six degree of freedom of 3D two-node beam element..... | 19 |
| Figure 16 (a) Timoshenko beam element showing shear deformation. Cross section area is no longer perpendicular to the neutral axis. (b) Two beam element meeting at node 2 (Logan, 2012)..... | 19 |
| Figure 17(a) Solid model before mesh and (b) after meshing (Steffen, 2012)..... | 20 |
| Figure 18 components of main window in ABAQUS..... | 23 |
| Figure 19 Uniform load on the flexible beam structure: (a) with free-end, (b) joined-both end (Ashby and Jones, 2012)..... | 28 |
| Figure 20 Set-up of the experiments (Gansel et al., 2013)..... | 31 |
| Figure 21 Geometry of PET net..... | 31 |
| Figure 22 Deformation of PET net in the x-direction at different flow speeds (Gansel et al., 2013) ... | 32 |
| Figure 23 Methodology flow chart..... | 35 |
| Figure 24 (a) Hexagonal shapes of a mesh and (b) PET net panel visualization in Part module..... | 36 |
| Figure 25 Diagonal and vertical section on a mesh with circular beam profile..... | 37 |
| Figure 26 (a) Seed with 0.01 m in size and (b) the model visualization after meshing (right)..... | 38 |
| Figure 27 Static general steps..... | 38 |
| Figure 28 (a) Region of applied loads and (b) load direction..... | 39 |
| Figure 29 Clamped boundary conditions..... | 40 |
| Figure 30 (a) Rotation and translation in vertical bar (b) Boundary conditions in the three nodes of the vertical bar: (b1) Case 1, (b2) Case 2, (b3) Case 3..... | 41 |
| Figure 31 Stress (S_{11}) versus Strain (E_{11})..... | 43 |
| Figure 32 Nodes at the position of sensor from SINTEF experiment..... | 43 |
| Figure 33 Comparison of deflection between cases and the experiment ($V1=0.13$ m/s)..... | 44 |

| | |
|---|----|
| Figure 34 Comparison of deflection between cases and the experiment (V2=0.25 m/s) | 44 |
| Figure 35 Comparison of deflection between cases and the experiment (V3=0.38 m/s) | 45 |
| Figure 36 Comparison of deflection between cases and the experiment (V4=0.5 m/s) | 45 |
| Figure 37 Comparison of deflection between cases and the experiment (V5=0.63 m/s) | 46 |
| Figure 38 Average coordinates of PET net panel from ABAQUS and experiment..... | 47 |
| Figure 39 Deformation of model in ABAQUS (F = 2.631 N, V = 0.13 m/s) | 49 |
| Figure 40 Deformation of model in ABAQUS (F = 6.922 N, V = 0.25 m/s) | 49 |
| Figure 41 Deformation of model in ABAQUS (F = 11.896 N, V = 0.38 m/s) | 50 |
| Figure 42 Deformation of model in ABAQUS (F = 17.922 N, V = 0.5 m/s) | 50 |
| Figure 43 Deformation of model in ABAQUS (F = 25.636 N, V = 0.63 m/s) | 50 |
| Figure 44 Deflection under different punctual loads: (a) 500N, (b) 2000N, (c) 5000N, (d) 10000N | 54 |
| Figure 45 Drag coefficient vs Reynolds number for long circular cylinders and spheres in cross flow (Sacks et al., 1963) | 55 |

List of Tables

| | |
|--|----|
| Table 1 Material classes (Ashby and Jones, 2012) | 3 |
| Table 2 Data for Young's modulus (Ashby and Jones, 2012) | 7 |
| Table 3 Aperture forms of net (Gansel et al., 2012) | 12 |
| Table 4 Beam element library in ABAQUS (Abaqus 6.11 doc) | 25 |
| Table 5 Load region..... | 29 |
| Table 6 Specification and dimension of PET net (Gansel et al., 2012)..... | 31 |
| Table 7 Material properties of PET net (Designerdata) | 32 |
| Table 8 Drag forces and its coordinate | 33 |
| Table 9 Distance displacement at each position | 33 |
| Table 10 Force per unit length calculation | 39 |
| Table 11 Modeling cases..... | 41 |
| Table 12 Experimental forces from SINTEF experiment and reaction forces from ABAQUS results at different flow speed..... | 42 |
| Table 13 Percentage of displacement error | 47 |
| Table 14 Average translation displacement for the different positions and under different loads..... | 48 |
| Table 15 Average rotation displacement at nodes for the different positions and under different loads..... | 51 |
| Table 16 Drag coefficient of the individual cylinder from the experiment | 55 |
| Table 17 Drag coefficient based theoretical calculation..... | 56 |

ABSTRACT

In this master thesis the structural modeling of Polyethylene Terephthalate (PET) net panel has been done using finite element software (ABAQUS). The model was built corresponding to the net panel experiment performed by SINTEF Fisheries and Aquaculture. The construction of the model was done by using Timoshenko beam element (B31) and performing static analysis.

The current forces from the experiment (2.63N, 6.9N, 11.9N, 17.99N and 25.6N) were simulated using line loads completely distributed over the net panel model. In addition, big challenges were found when constructed the vertical bar due to the complex geometry of PET net, for that reason the model was simplified in the vertical bar.

The displacements of the model were bigger with increasing the applied load, same reaction as the experiments. While comparing the results with the experiment it was found that the ABAQUS model had a good matching at bigger loads. However it is was concluded that the model can structurally simulate in a good grade the behavior of the net panel from the experiment.

CHAPTER 1

INTRODUCTION

1.1 Background

The growth of the fish farm industry in Norway over the past decades was supported by new designs and materials for aquaculture, allowing bigger fish cages to be located in more exposed areas. Open sea or exposed area raise to many challenges to the fish farm due to rough environmental conditions. High waves and strong surface current may cause the fish cages collapsed and fish escapes. Thus, these challenges are under consideration for the new development of fish cages design and material (Gansel et al., 2013).

Some fish cage net materials have been proposed in order to improve the stability of the cages under the action of current and waves. Net material made from nylon is the most common material that has been used in the fish farms. Even though Nylon has essential benefits such as; lightweight, flexible, and relatively low cost, Nylon shows also some deficiencies due to its poor resistance to the abrasion, limited tensile strength, wear and tear and degradation of several of the mechanical properties with time (Gansel et al., 2013). Therefore, new materials have been introduced; steel, Polyethylene Terephthalate (PET) copper and alloy.

When net cage is exposed to strong current, the shape is changed by deflection and deformation. This leads to decrease in cage volume and affects the structural integrity and stability of the net structure (Tsukrov et al., 2011). Hence, advancements in the engineering analysis of nets are needed to improve design, performance and reliability of net structures. The behavior of net in current and waves is one of the important factors to be analyzed. Gansel et al., (2013) conducted experimental and numerical studies on the deformation of net panels (steel, copper, PET) to outline the performance of each net due to normal uniform current.

1.2 Objectives

Since the increase in demand for fish, aquaculture has been expanding rapidly. In many countries the coastal aquaculture is faced with strong resistance from other industries and therefore the aquaculture industry has to move into more open waters. Moving into more exposed areas require alternative technology and material for the design of the fish cages. Therefore, recently there have been many studies with regard to different materials used for nets. Due to complexity of the net-cage system it is not always easy to study the

behavior of the net cage system analytically. In most cases complicated numerical simulations need to be developed and verified through experiments. However, some net materials such as PET are a very stiff material and have little localized deformation compared to the commonly used nylon net. Therefore, it is hypothesized that deformation of stiff net like PET can be predicted by simple structural analysis, instead of using complicated hydrodynamic models. Therefore, the objectives of this study are to:

- Construct the PET net panel model in ABAQUS corresponding to the net specifications in SINTEF experiment (Gansel et al., 2013).
- Analyze the bending of the net panel at various loads that corresponds to different current velocities in the experiment.
- Comparison of the result between ABAQUS and SINTEF experiment to determine if simple structural analysis can predict the bending or deformation of the net panel.

1.3 Scope of Work

The scope and motivation for this thesis is to gain knowledge and understanding of structural modeling of net panels and thus to analyze the response of the panel while it is under different loads. The net use is a net made from PET material which is not as flexible as nylon and it has not been so much studied until now. Therefore this was an interesting challenge for us.

After modeling the net panel response, it would be compared with SINTEF experiment performed with the same material. Although it may be considered that this is a simplification but can give an insight into the loads of the net. However, the total response of a fish farm cage must take all system components into account which are not analyzed as part of this work.

CHAPTER 2

NET MATERIAL

2.1 Net Types

Due to their properties, several materials have been used for aquaculture net cage. In Table 1, it can be seen the classes of material which are commonly used in aquaculture. Nylon (PA) being the material that has been traditionally used by the industry and, it is also the most extensively studied.

Table 1 Material classes (Ashby and Jones, 2012)

| | |
|-----------------------------|---|
| Metals and alloys | Iron and steels |
| | Aluminum and alloys |
| | Copper and alloys |
| | Nickel and alloys |
| Polymers | Polyethylene (PE) |
| | Nylon or polyamide (PA) |
| | Polyethylene Terephthalate (PET) |
| Ceramics and glasses | Silica (SiO ₂) glasses and silicates |
| | Silicon carbide (SiC) |
| | Silicon nitride (Si ₃ N ₄) |

Nylon materials, Figure 1 (h) and 1(i), has been studied in some experiments conducted by Aarsnes et al. (1990), Tsukrov et al. (2011), Kristiansen and Faltinsen (2012), Gansel et al. (2012), Moe et al. (2010) and many others. However due to new materials that have been introduced into the aquaculture, it has become also necessary to study their behavior, thus Net panel with steel, copper, and PET in Figure 1 (a) and 1(c) were tested in the experiment of Gansel et al. (2012) and Jensen et al. (2013). Other materials of net were also studied by Tsukrov et al. (2011) such as: expanded copper-nickel (made of 90% copper and 10% nickel), chain-link woven brass (65% copper and 35% zinc), welded silicon-bronze and woven silicon-bronze (composed of 97% copper and 3% silicon) show in Figure 1 (d) and 1(g).

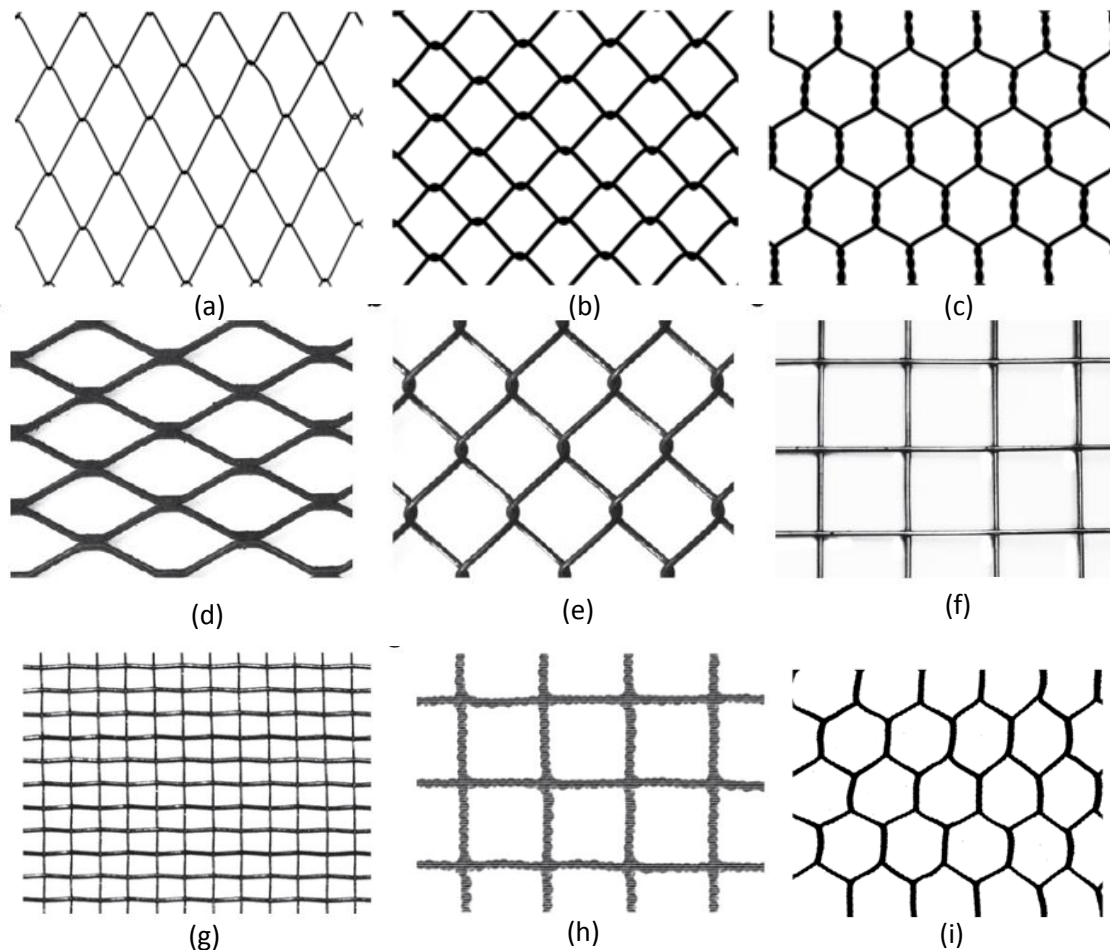


Figure 1 Types of aquaculture net: (a) steel net, (b) copper net, (c) PET net, (d) Flattened expanded copper-nickel, (e) Chain-link woven brass, (f) Welded silicon-bronze, (g) Woven silicon-bronze, (h) Nylon knotless square net, (i) Nylon015 (Tsukrov et al., 2011), (Gansel et al., 2012).

Studies of net materials have been carried out to measure the capability of net in different load conditions. In this context Gansel et al. (2013) found that the elasticity of net material, its construction, its density of material, drag properties due to mesh bar thickness, solidity, geometry and initial permanent deformation influenced the deformation over net panel with bending stiffness.

The capability of new net materials to contain farmed fish is required by legislation (Norwegian Ministry of Fisheries and Coastal Affairs, 2011), which is enforced by a technical standard (Norwegian Standard, 2009). Standard Norge (2009) states that a main component shall be dimensioned in order to:

- Function satisfactory based in a given assumptions, such as environmental forces
- Tolerate all assumed loads, including deformations, with satisfactory protection against breaking
- Show satisfactory protection against an undesirable event triggering a more significant event than the triggering event itself

- Show satisfactory resistance to mechanical, physical, chemical and biological effects, seen in relation to design working life.

Regarding the material characteristic, it is also noted in the Norwegian Standard (2009) that if a material characteristic is not provided, it shall be found by relevant, standardized test under defined and relevant conditions. In addition, a conversion factor shall be used if necessary so that the test results are representative of the material characteristics and the relevant construction. A characteristic capacity has a given probability for not being under-reached in an unlimited series of tests. Thus it indicates a material characteristic and is defined as the mean value for rigidity parameter.

2.2 Material Properties

Material properties determine the response of a structure to the applied loads. Physical properties (density) and mechanical properties (Young's modulus, yield and tensile strength, fatigue strength, Poisson's ratio) of material are important and have to be considered in structural analysis.

Density is defined as mass per unit volume and determines submerged weight in the water. Gansel et al. (2012) found an indication that density is important for deformation of nets with bending stiffness due to the balance between drag and gravitational force. Hence the combination among material density, bending stiffness and drag properties will determine the deformation.

Mechanical properties of material include important properties as described below (Rajput, 2005):

1. *Strength* – the ability of material to withstand various forces without bending, breaking, shattering or deforming in any way.
2. *Elasticity* – perfectly elastic if the whole of the stress produced by a load disappears completely on the removal of the load, modulus of elasticity of Young's modulus (E) is proportionally constant between stress and strain for elastic material. Young's modulus indicates stiffness.
3. *Plasticity* – the property that enables permanent deformation in a material even after the load is removed.
4. *Ductility* – the ability of material to withstand elongation or bending (change shape). The material shows a considerable amount of plasticity during the ductile extension.
5. *Malleability* – the property by virtue of which a material may be hammered or rolled into thin sheets without rupture.
6. *Toughness (tenacity)* – the ability of material to oppose rupture.
7. *Brittleness* – lack of ductility and brittle will occur when body easily break
8. *Hardness* – resistance of material to penetration

9. *Fatigue* – occur when subjected to fluctuating loads and material tend to develop characteristic behavior which is different from that (or materials) under steady loads.
10. *Creep* – slow plastic deformation of metals under constant stress.

Any material may fail if is not able to withstand the external load (Figure 2). Therefore, successful design of structure requires structural analysis in order to ensure such that material be able to support structure from applied load (Jianqiao, 2008). Structural design must consider the following aspect to avoid failure (Jianqiao, 2008):

1. Strength – the structure must be strong enough to withstand from applied load
2. Stiffness – the structure must be stiff enough such that only allowable deformation occurs
3. Stability – the structure must not collapse through buckling

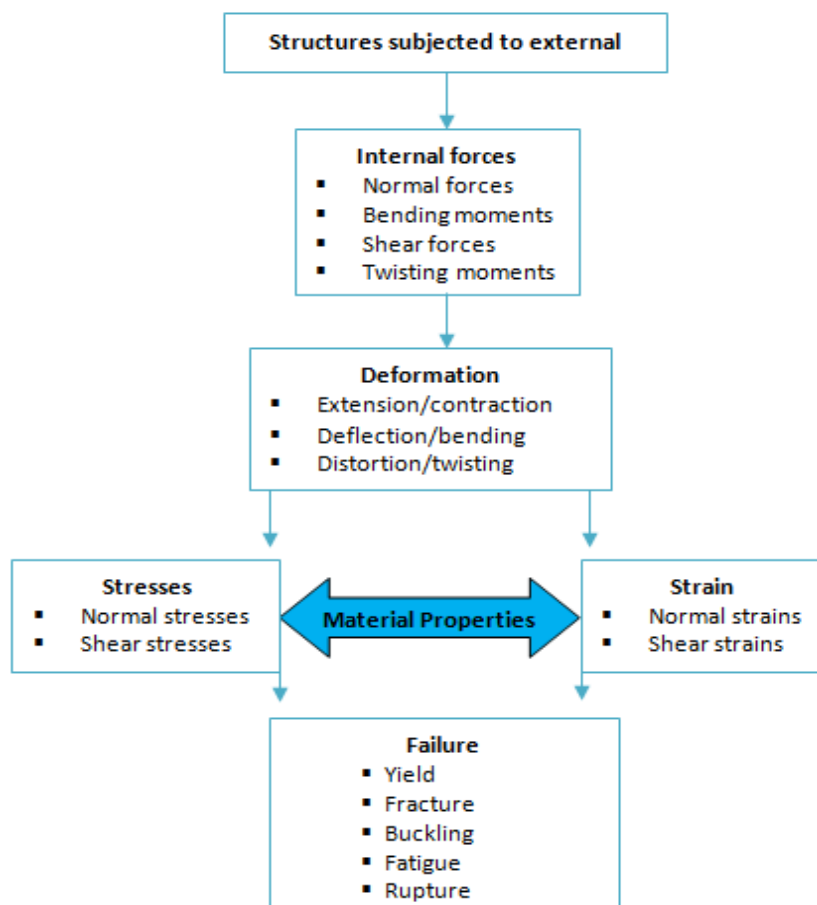


Figure 2 Structural behavior due to external loads (Jianqiao, 2008)

Bending Stiffness

Basically bending stiffness (EI) can be determined from modulus of elasticity (E) and second moment of inertia (I) of a beam cross section and can be expressed in Equation 2.1. Modulus measures the resistance of a material to elastic deflection.

$$M = EI\kappa = EI \frac{\partial^2 w}{\partial x^2} \tag{2.1}$$

Where w is the deflection and x is its coordinate. Small values of E reflect flexible material and large values indicate rigid material. Young’s modulus used in the finite element analysis is a type of modulus of elasticity that describes tensile elasticity. Range values of Young’s modulus for various materials are presented in Table 2.

Table 2 Data for Young's modulus (Ashby and Jones, 2012)

| Material | E (GN/m ²) |
|----------------------------------|------------------------|
| Mild steel | 200 |
| Copper | 124 |
| Copper alloys | 120-150 |
| Polyethylene | 0.7 |
| Polyethylene Terephthalate (PET) | 2.7-3.1 |
| Nylon | 2-4 |
| Polyamide | 3-5 |

Although the material of PET net has modulus elasticity, the complex geometry of the net will significantly influence the bending stiffness. In addition, bending stiffness on net material influences the behavior of the net significantly while exposed to hydrodynamic loads. Forces and deformation on the net are affected by bending stiffness (Gansel et al., 2013).

Stress definition

Stress is a result of forces (F) which are acting on the specific area (A), giving the following Equation 2.2:

$$\sigma = \frac{F}{A} \tag{2.2}$$

When the forces act normal to the area and with different direction, it is called tensile stress. Practically, the forces are commonly working with an angle to the section area and in order to solve it the forces are divided into two components; normal to the surface (F_t), and parallel to it (F_s). F_t creates a tensile stress and F_s cause shear stress (Figure 3). Each magnitude of the stress is given in Equation 2.3 & 2.4 (Ashby and Jones, 2012).

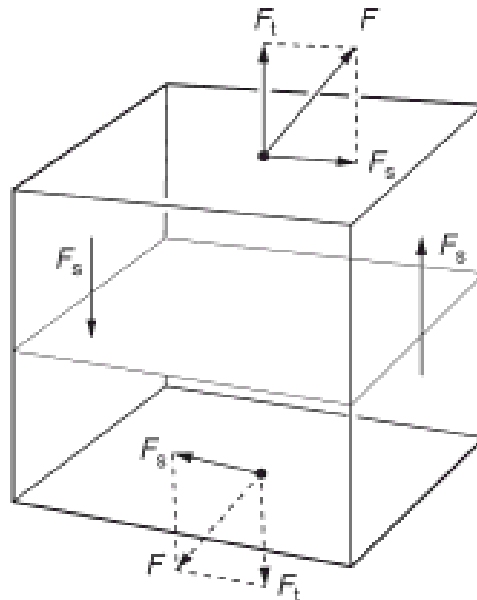


Figure 3 Definition of stress (Ashby and Jones, 2012)

$$\text{Tensile stress: } \sigma = \frac{F_t}{A} \quad (2.3)$$

$$\text{Shear stress: } \tau = \frac{F_s}{A} \quad (2.4)$$

The state of stress which is commonly occurring is simple tension and compression as can be seen in Figure 4.

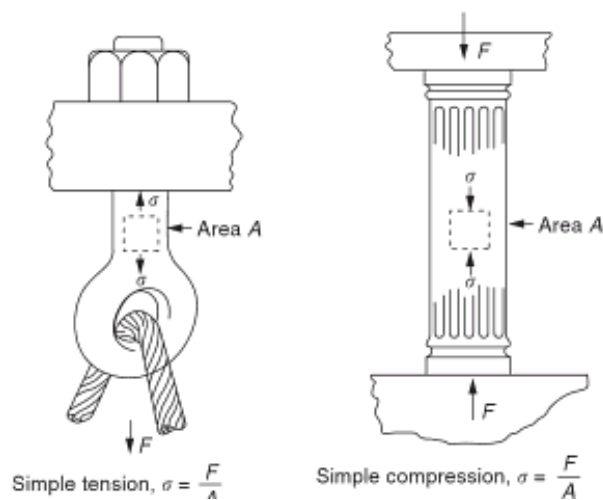


Figure 4 Simple tension and compression (Ashby and Jones, 2012)

The equation for von Mises stress allows the most complex stress situation to be presented by a single quantity (Budynas and nisbett, 2010). Steffen (2012) concluded that for the most complex state of stress (e. g., a three-dimensional stress element subject to a combination of shear and normal stresses acting on every faces, as presented in Figure 5). The number of von Mises stress represents stress magnitude which is comparable against yield strength

and ultimate tensile strength of the material to measure failure occurrence. The von Mises stress is always positive as scalar number.

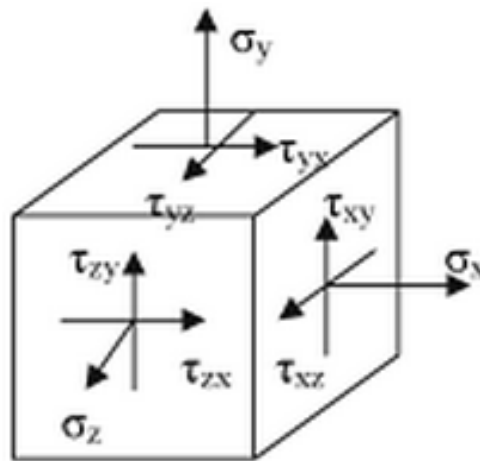


Figure 5 three-dimensional stress element subjected to a combination of stress (Steffen, 2012)

Strain definition

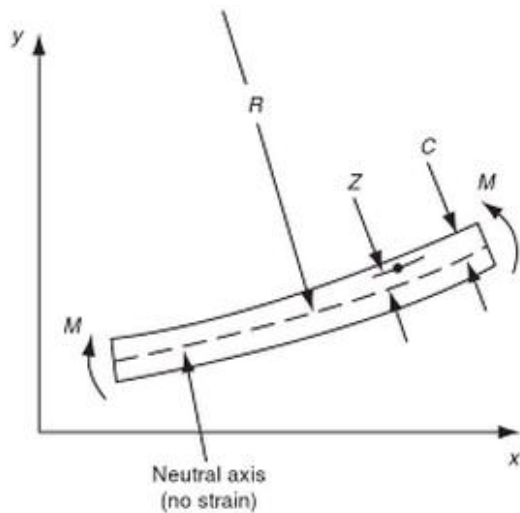
The materials will respond to the stress by straining. Under a given stress, a stiff material strains only slightly, a floppy or compliant material (e.g. polyethylene) strain much more (Ashby and Jones, 2012). Tensile stress induces a tensile strain. If the structure with side l extends in u amount parallel to the tensile stress, the tensile strain can be formulated below:

$$\epsilon_n = \frac{u}{l} \quad (2.5)$$

When the structure strains, it will get thinner and the amount of shrink inward is represented by the Poisson's ratio (ν). The Poisson's ratio is a negative ratio of the inward strain and original tensile strength (Ashby and Jones, 2012):

$$\nu = -\frac{\text{lateral strain}}{\text{tensile strain}} \quad (2.6)$$

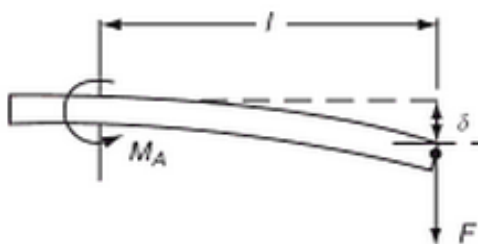
To measure strain, a bar can be loaded in bending and the equations that describe the relation between applied load and deflection for elastic beams can be illustrated in figure below (Figure 6).



$$\sigma = \frac{Mz}{I}$$

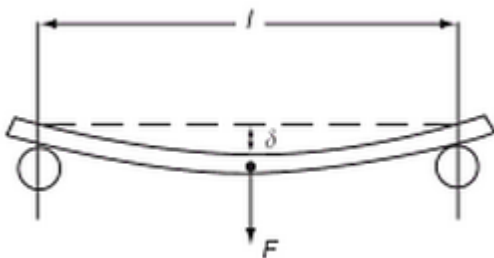
$$\sigma_{\max} = \frac{Mc}{I}$$

$$\frac{d^2y}{dx^2} = \frac{1}{R} = \frac{M}{EI}$$



$$\delta = \frac{1}{3} \left(\frac{Fl^3}{EI} \right)$$

$$M_A = Fl$$



$$\delta = \frac{1}{48} \left(\frac{Fl^3}{EI} \right)$$

Maximum moment is $\frac{Fl}{4}$ at mid span

Figure 6 elastic bending of beams (Ashby and Jones, 2012)

Where σ is the stress induced by bending, l represent the length of beam, R is the radius of curvature, F , δ , M , E , and I are applied force, displacement, bending moment, Young's modulus, and second moment of inertia, respectively.

Stress and strain calculation is usually used to see the elasticity of the structure during analysis. If the plot of stress and strain shows linear relation, the analysis is assumed as linear elastic. Figure 7 illustrates the linear region in the stress-strain curve.

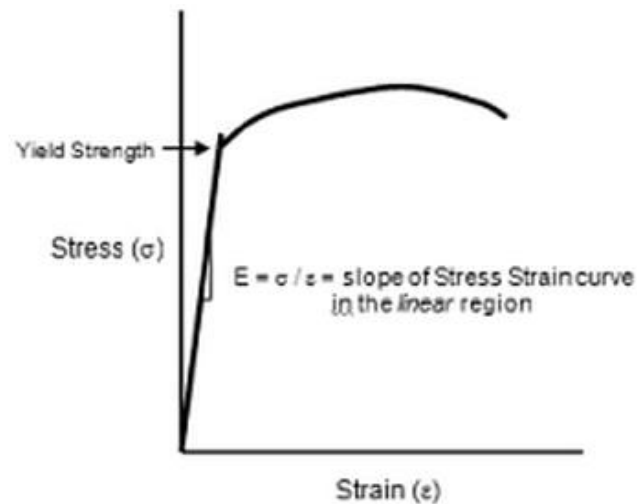


Figure 7 Stress-strain curves (Steffen, 2012)

2.3 Net Geometry

As can be seen in Figure 1 the geometry of the nets differ in aperture and joined; the aperture form of nets varies from diamond to hexagonal and the join or link has different features such as: knot, knotless, chain, welded, spiral twisted (Table 3). This becomes a challenge when modeling the net in software if the detail of geometry has to be present. Vertical section of PET net is constructed by two net twines that tie each other forming spiral feature (Figure 8). As a result of this spiral feature, the vertical section is thicker than other section of PET net and allowing rotation between the mesh up to 360° . This structural difference can affect the water flow through the net or the dependency Re of drag coefficient (Gansel et al., 2012).

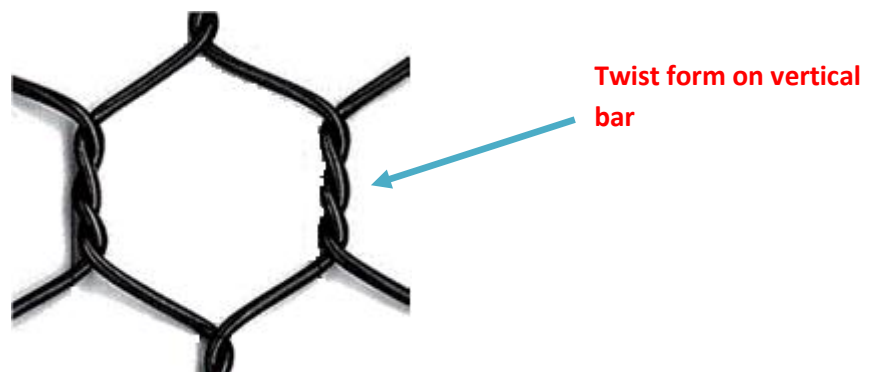


Figure 8 PET net geometry

Table 3 Aperture forms of net (Gansel et al., 2012)

| Type of net | Aperture form |
|-------------|---------------|
| Steel net | Diamond |
| Copper net | Diamond |
| PET net | Hexagonal |
| Nylon 015 | Hexagonal |

Different net material shows different response when is subjected to loads, even if has been built with similar geometry feature. Gansel et al. (2012) showed PET net has stronger variation of C_D with change in flow speed although has similar solidity, aperture form and aperture size as Nylon net.

The advantages of PET net can be summarized as follows (AKVAGroup, 2011-2012):

- High durability
Has 20-years lifespan compared to Nylon net that often last 4-7 years
- Escape prevention
- Maximized water flow
- No need for antifouling paint
- Easily recyclable material

CHAPTER 3

FINITE ELEMENT METHOD

3.1 Introduction

Finite element method (FEM) is defined as a procedure for the numerical solution of the equations that govern the problems in nature. The behavior of nature is usually described in differential or integral form. FEM may allow the evolution in space and/or time of one or more variables representing the behavior of a physical system (Onate, 2009). In Figure 9 it is illustrated a general procedure of FEM for a structure in a computational model.

According to Sævik et al. (2010) finite element method is based on 3 principles as mentioned below:

1) *Equilibrium*

There are equilibrium in forces and moments.

2) *Kinematic compatibility*

All adjacent cross sections will have the same displacement and deformation and will continue as it deforms. No cracks will occur and the strain will be finite.

3) *Material law*

Stress - strain relationship. According to Hooke's law $\sigma = E\epsilon$

The basic idea of the finite elements is to break up a continuum into discrete number of smaller "elements". These elements can be modelled mathematically by a stiffness matrix and are connected by nodes that have degrees of freedom. The result of the finite element is to create a stiffness matrix and a set of loads. Below there is listed a typical FEM process (Quek and Liu, 2003):

- Divide structure into pieces (elements with nodes)
- Describe the behaviour of the physical quantities on each element
- Connect (assemble) the elements at the nodes to form an approximate system of equations for the whole structure
- Solve the system of equations involving unknown quantities at the nodes (e.g., displacements)
- Calculated desired quantities (e.g., strains and stresses) at select elements

As mentioned above, Quek and Liu (2003) explained when using FEM to solve mechanic problems governed by a set of partial differential equations, the first main problem is to discretize into small elements. Each of these elements, the profile of the displacements is assumed in simple forms to obtain element equations. These element equations are then

assembled together with adjoining elements to form the global finite element equation. The equation for the global main problem can be solved easily for the entire displacement field.

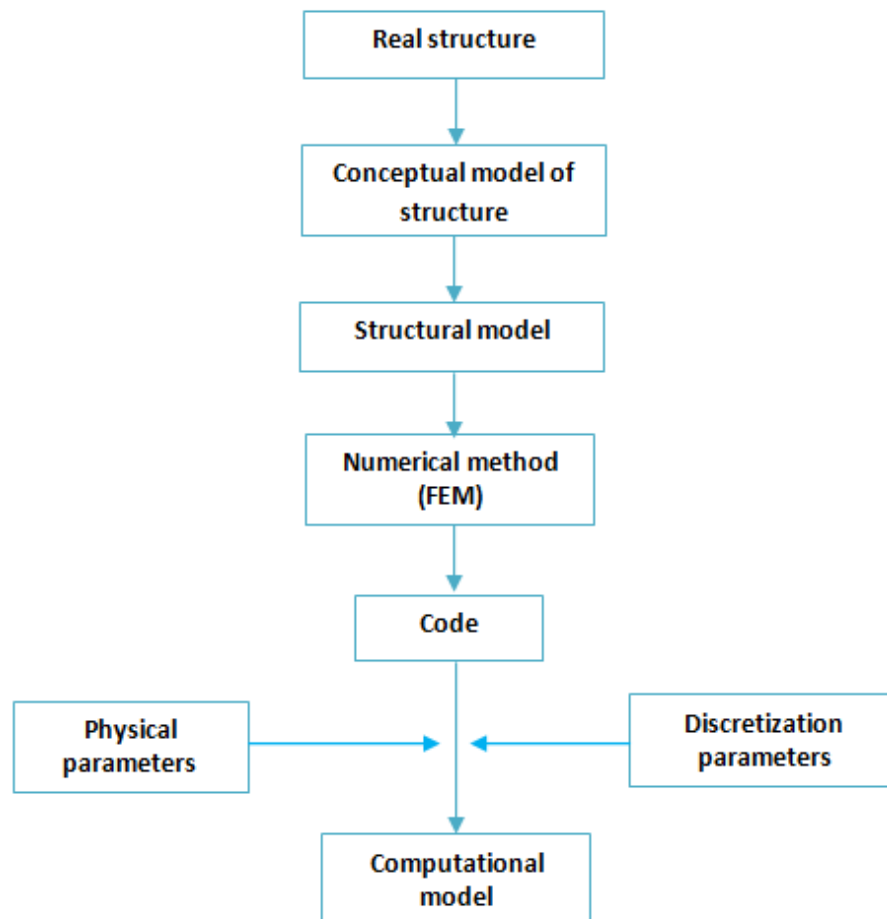


Figure 9 FEM paths from the real structure to the computational model (Onate, 2009)

The geometry of the structure is discretized or divided into finite elements of certain accuracy. During finite element analysis process there are three errors categories which commonly occur: modeling error, discretization error, and numerical error (Onate, 2009). The modeling error can be reduced by improving the conceptual and structural models considering the actual behavior of the structure. The discretization error can be reduced by using finer mesh (i.e. more elements), or increasing the accuracy of finite elements by using higher order polynomial expansions for the approximation of displacement field within each element. Numerical errors are introduced by the use of computer. This error is usually small and associated with the ability to represent data accurately with numbers of finite precision (Onate, 2009).

For analyze structure such as frames, buildings, foundation, retaining walls, bridges, etc., can be use the following structural models as shown in Figure 10.

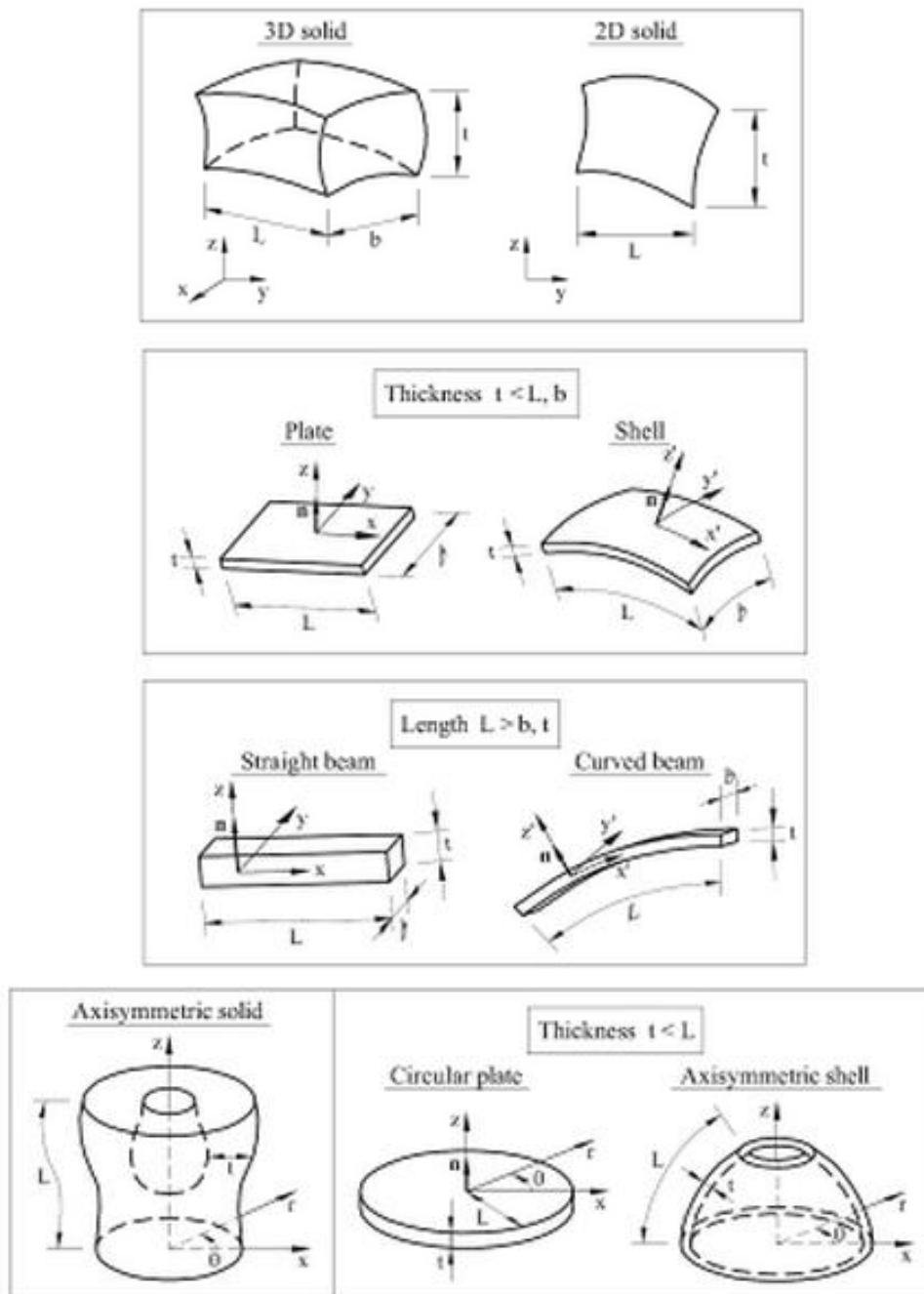


Figure 10 Structural models (Onate, 2009)

3.2 Nodes, Elements, and Degree of Freedom

Mathematical analysis in finite element method requires simplification of modeled part. In the case of a cylindrical structure, it is divided into number of nodes and elements as shown in Figure 11.

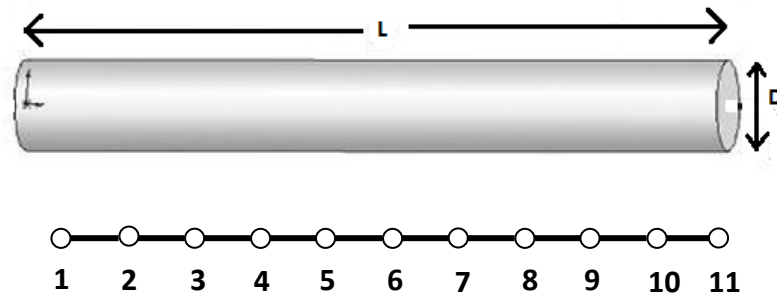


Figure 11 Cylindrical structure is subdivided into a series of node and elements (Steffen, 2012)

In Figure 11 Nodes are represented by the point circle with number and in the connection between lines. Elements are defined by the short line segment between the nodes. The number of nodes and elements it will be given in any FEM software.



Figure 12 A one-dimensional model (2-nodes and one element) represent its displacement ($U_{x(n)}$ & $U_{x(n+1)}$) in x-direction (Steffen, 2012)

A simple one-degree of freedom elements is shown in Figure 12. Steffen (2012) explained that the assumption of displacement in two nodes (n & n+1) that lies in the x-direction ensures that the problem is one-dimensional (i.e., the displacement is only allowed in one-direction). $U_{x(n)}$ and $U_{x(n+1)}$ are the displacements in the x-direction and these displacements correspond to one-degree of freedom at each node. Each node results in one set equation and it can be concluded that one element in Figure 12 has two sets of equations. For the structure in Figure 11 with two nodes in one element, the total number degrees of freedom are:

$$(10\text{elements}) * (2\text{nodes/elements}) * (1\text{dof / node}) = 20\text{dof}$$

3.3 Beam Element

Beam element is a slender structure and has uniform cross section. Beam element is commonly used as structural component and geometrically a straight bar, which only deform in perpendicular direction of its axis. The main difference between beam and truss is the type of carried load. Beams are subjected to the transverse loading, including transverse force and moments that result in transverse deformation (Quek and Liu, 2003).

Euler –Bernoulli beam element

Euler-Bernoulli beam theory is used for thin beam. In planar beam elements there are two degrees of freedom (DOFs) at a node in its local system; deflection in the y direction, v , and the rotation in the x - y plane, θ_z with respect to the z -axis as can be seen in Figure 13. Therefore, each beam element has four degree of freedom (Quek and Liu, 2003).

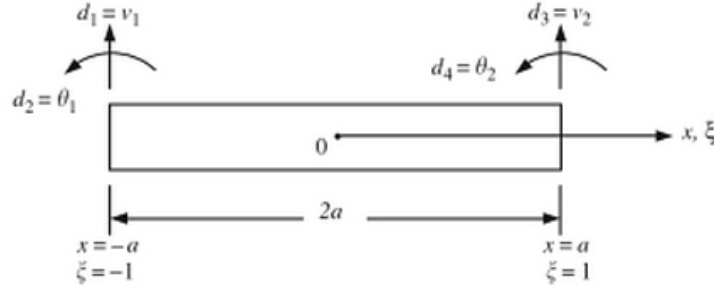


Figure 13 Beam element with its local coordinate system: physical coordinates x , natural coordinate ξ (Quek and Liu, 2003).

Logan (2012) explained the differential equations governing elementary linear-elastic beam behavior (Euler-Bernoulli beam), which is based on plane cross sections perpendicular to the longitudinal centroidal axis of the beam before bending occurs, remaining plane and perpendicular to the longitudinal axis after bending occurs. Figure 14 shows a plane through vertical line a - c (Figure 14a) is perpendicular to the longitudinal axis before bending, and this plane through a' - c' (rotating through angle ϕ in Figure 14b) remains perpendicular to the bent x axis after bending. Practically, this occurs only when a pure couple or constant moment exists in the beam. However, it is reasonable assumption that yields equation that is able to predict beam behavior accurately.

Consider the beam as shown in Figure 14 that is subjected to a distributed loading $w(x)$ (force/length). Figure 14c) illustrated the differential element of the beam and its force and moment equilibrium can be formulated as follows:

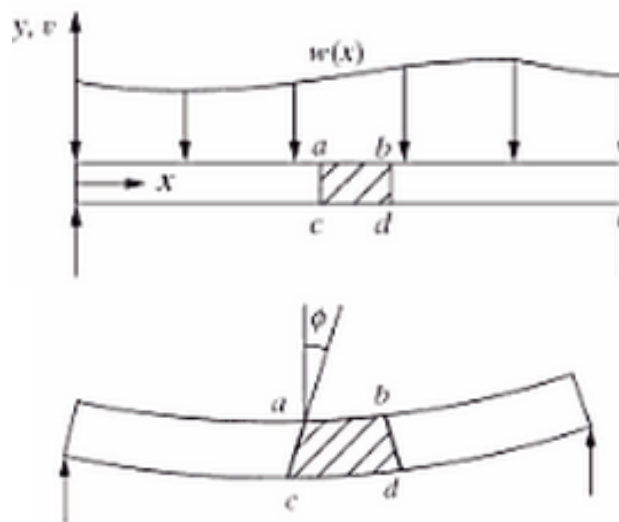
$$\sum F_y = 0: V - (V + dV) - w(x)dx = 0 \quad (3.1)$$

Or can be simplified as:

$$- wdx - dV = 0 \text{ or } w = -\frac{dV}{dx} \quad (3.2)$$

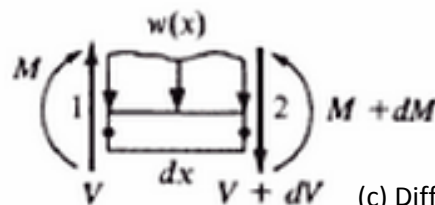
$$\sum M_2 = 0: -Vdx + dM + w(x)dx \frac{dx}{2} = 0 \text{ or } V = \frac{dM}{dx} \quad (3.3)$$

The final result related to the shear force, to the bending moment is obtained by dividing the left equation by dx and then take the limit of the equation as dx approaches 0, so that the term $w(x)$ is deleted.



(a) Undeformed beam under the load $w(x)$

(b) Deformed beam due to beam applied loading



(c) Differential beam element

Figure 14 Beam under distributed load (Logan, 2012)

Timoshenko Beam element

A three-dimensional Timoshenko beam element has two nodes with six degrees of freedom at each node (Figure 15). The shear deformation (deformation due to the shear force V) is now included instead of plane sections remaining plane after bending occurs as mentioned previously. The shear deformation beam theory is used for this case (Logan, 2012).

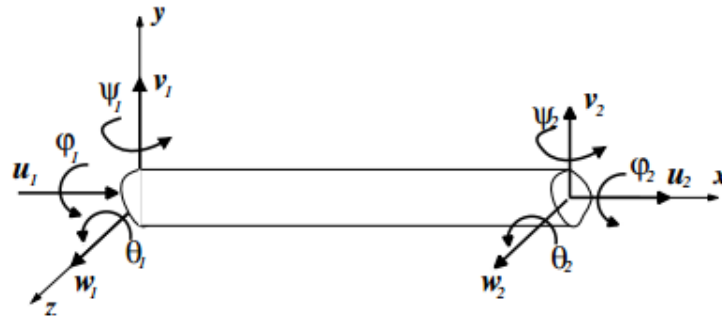


Figure 15 Six degree of freedom of 3D two-node beam element

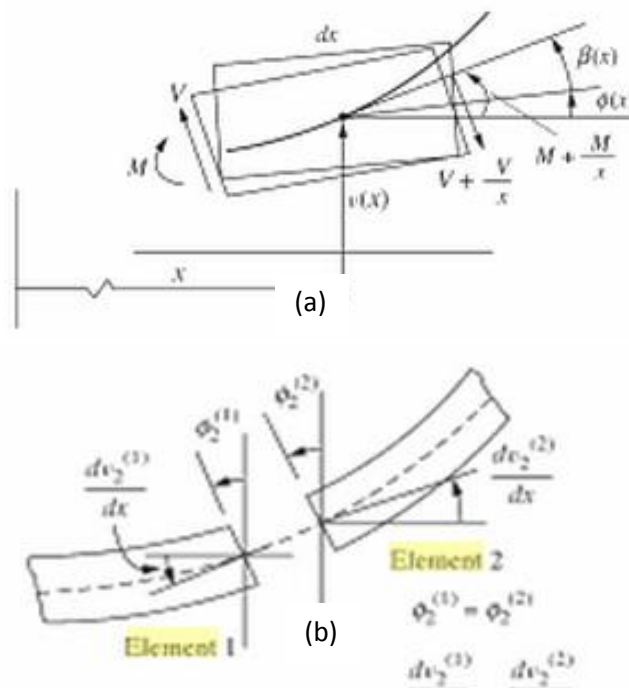


Figure 16 (a) Timoshenko beam element showing shear deformation. Cross section area is no longer perpendicular to the neutral axis. (b) Two beam element meeting at node 2 (Logan, 2012)

Figure 16 shows a section of a beam of differential length dx , assuming the cross section to remain plane but no longer perpendicular to neutral axis. This is due to the inclusion of shear forces which results in a rotation term indicated by β . The total deflection of the beam at a point x now consists of two parts, one caused by bending and one by shear force (Logan, 2012). Hence, the deflection curve at point x can be written as:

$$\frac{dv}{dx} = \phi(x) + \beta(x) \tag{3.4}$$

Where $\phi(x)$ is the rotation due to bending moment and $\beta(x)$ is the rotation due to transverse shear force. Logan (2012) assumed linear deflection and angular deflection (slope) are small. The correlation between bending moment and bending deformation (curvature) can be defined as:

$$M(x) = EI \frac{d\phi(x)}{dx} \quad (3.5)$$

The relation between the shear force and shear deformation (rotation due to shear) or shear strain is shown by the following formula

$$V(x) = k_s AG\beta(x) \quad (3.6)$$

The difference in dv/dx and ϕ represent the shear strain γ_{yz} ($=\beta$) of the beam element as

$$\gamma_{yz} = \frac{dv}{dx} - \phi \quad (3.7)$$

Several two-node Timoshenko beam finite element has been described by Hughes et al. (1977) that used linear Lagrange polynomials for displacement and rotation, MacNeal (1976) used also linear Lagrange poly-nomials for the displacement and rotation, but has an additional correction called 'residual bending flexibility', and Tessler and Dong (1981) used full numerical integration with a quadratic polynomial for the displacement and a linear polynomial for the rotation, where the shape functions are interconnected to prevent 'shear-locking'.

3.4 Mesh

Meshing is the process of subdividing structural elements into an organized set of nodes and elements (Figure 17). This imply to the mathematical solution of finite element analysis which depends set of simultaneous equations that describe small displacement at element level (Steffen, 2012).

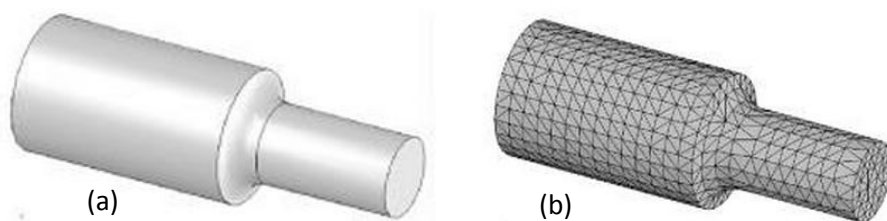


Figure 17(a) Solid model before mesh and (b) after meshing (Steffen, 2012)

3.5 Formula

Finite element analysis has been performed using two formulations: Lagrangian and Eulerian. In Lagrangian formulation the nodes are associated with material points and analysis follows the material points. Eulerian formulation defines that the nodes are fixed in space and material points move through the mesh (Coutinho and Mayne, 2013). Lagrangian formulation is usually used for solid and Eulerian formulation is applied for fluid.

Markopoulos (2013) found that the disadvantage of Lagrangian formulation is connected to the large mesh deformation observed during simulation. Due to the attachment of the mesh on the work piece material, the mesh is distorted because of the plastic deformation in the cutting zone. This distortion may result in the failure of the model as it cannot be handled by the element applied in the mesh.

In ABAQUS/Standard, some element families have a standard formulation (Lagrangian and Eulerian) as well as some alternative formulations (Abaqus 6.11 doc). For example, the continuum, beam, and truss element families include members with a hybrid formulation (to deal with incompressible or inextensible behavior); these elements are identified by the letter H at the end of the name (C3D8H or B31H).

3.6 Static Analysis

Static analysis consists of solution of the equilibrium equation and resulting in displacement and stress as the output. Quek and Liu (2003) described that all individual elements can be assembled together to form the global FE system equation (Eq. 3.8):

$$KD + M\ddot{D} = F \quad (3.8)$$

In static analysis the term global mass matrix \mathbf{M} is neglected. Hence, the equation for static system can be simplified as in Eq. 3.9:

$$KD = F \quad (3.9)$$

Where \mathbf{K} is the global stiffness matrix, \mathbf{D} is a vector of all the displacements at all the nodes, and \mathbf{F} represents a vector of all equivalent nodal force vectors

In ABAQUS/standard and ABAQUS/CAE static stress analysis is used when inertia effects may be neglected and can be used for linear or nonlinear analysis (Abaqus 6.11 doc, Section 6.2.2). Linear static analysis involves the specification of load cases and appropriate boundary conditions. Nonlinear analysis is used for nonlinearities that arise from large-displacement effects, material nonlinearity, and/or boundary nonlinearities such as contact and must be accounted for.

During static analysis in Abaqus, boundary conditions can be applied to any of the displacement or rotation degrees of freedom (1–6). The element output for a static stress analysis includes stress, strain, composite failure measures and energies (values of state, field, and user-defined variables). The nodal output available includes displacements, reaction forces, and coordinates (Abaqus 6.11 doc, Section 6.2.2).

3.5 ABAQUS Software

ABAQUS is a suitable software application for finite element analysis and computer-aided engineering. The ABAQUS finite element system includes (Abaqus 6.11, section 1.1.1):

- ABAQUS/Standard, a general-purpose finite element program;
- ABAQUS/Explicit, an explicit dynamics finite element program;
- ABAQUS/CFD, a general-purpose computational fluid dynamics program;
- ABAQUS/CAE, an interactive environment used to create finite element models, submit ABAQUS analyses, monitor and diagnose jobs, and evaluate results; and
- ABAQUS/Viewer, a subset of ABAQUS/CAE that contains only the post processing capabilities of the Visualization module.

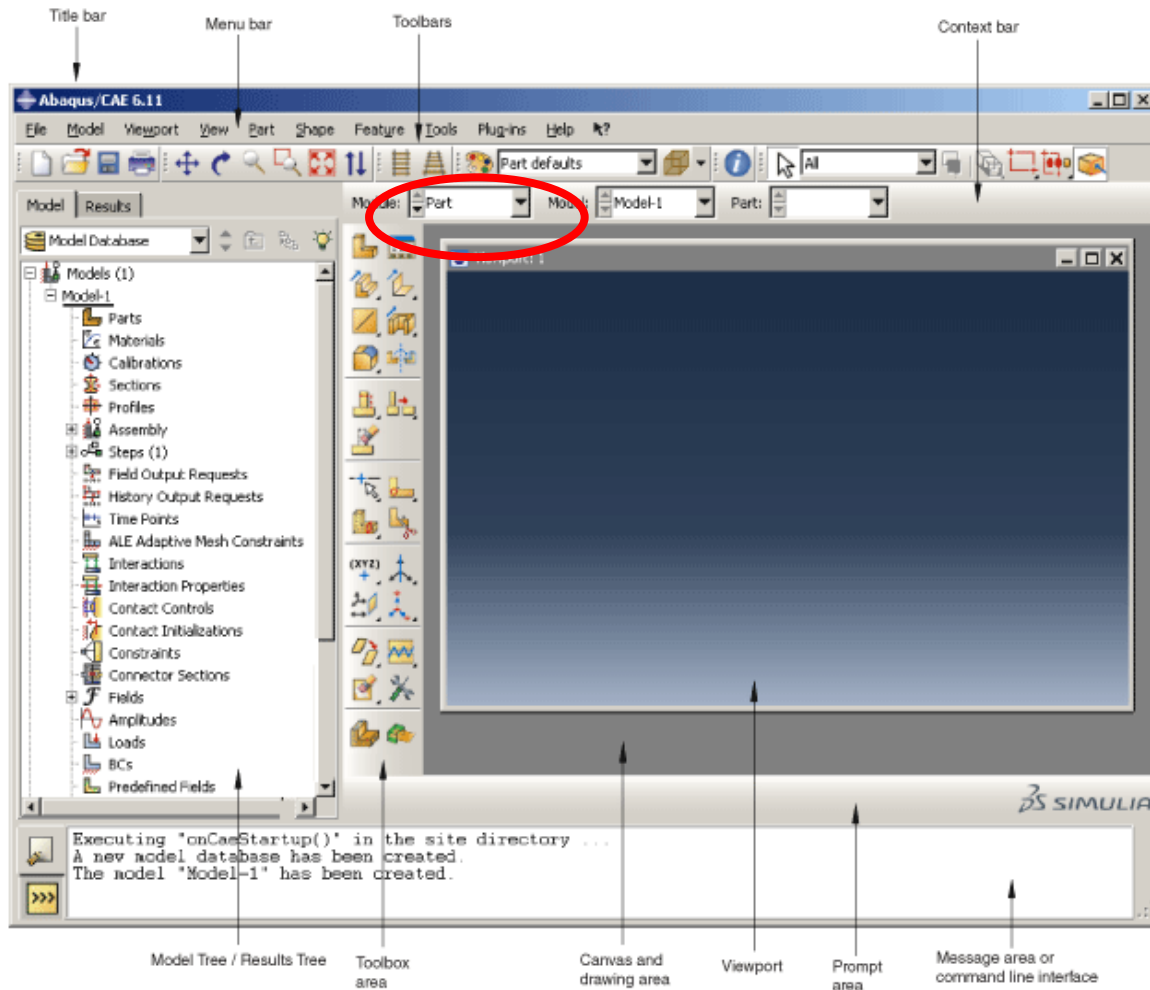


Figure 18 components of main window in ABAQUS

Abaqus/CAE is divided into functional units called modules (identified in the red circle in Figure 18). Each module contains only tools that are relevant to a specific portion of the modeling task. In each following module, Abaqus user is able to perform modeling task as described briefly below (Abaqus 6.11 documentation, section 2.3):

1) Part

Create individual parts by sketching or importing geometry.

2) Property

Create section and material definitions and assign them to region of parts.

3) Assembly

Create and assemble part instances.

4) Step

Create and define analysis steps and associated output request.

5) Interaction

Specify the interactions, such as contact, between regions of a model

6) Load

Specify loads, boundary conditions, and fields. In the static stress analysis the load can be applied as concentrated loads and distributed loads.

7) Mesh

Create finite element mesh. The mesh can be defined either on a part or on an instance of that part (not both). If the mesh is defined on a part, it is inherited by every instance of that part.

8) Optimization

Create and configure an optimization task.

9) Job

Submit a job for analysis and monitor shows its progress.

10) Visualization

View analysis result.

11) Sketch

Create two-dimensional sketches.

Beam element

In ABAQUS a beam element is a one-dimensional line element in three-dimensional space or in the X - Y plane that has stiffness associated with deformation of the line (the beam's "axis"). These deformations consist of axial stretch; curvature change (bending); and, in space, torsion. Truss elements are one-dimensional line elements that have only axial stiffness. Beam elements offer additional flexibility associated with transverse shear deformation between the beam's axis and its cross-section directions (Abaqus 6.11 doc, Section 28.3.1).

The ABAQUS/Standard beam element library includes following beam types (Abaqus 6.11 doc, Section 28.3.3):

- Euler-Bernoulli (slender) beams in a plane and in space;
- Timoshenko (shear flexible) beams in a plane and in space;
- Linear, quadratic, and cubic interpolation formulations;
- Warping (open section) beams;
- Pipe elements; and
- Hybrid formulation beams, typically used for very stiff beams that rotate significantly (applications in robotics or in very flexible structures such as offshore pipelines).

Available beam element (Euler-Bernoulli and Timoshenko) in Abaqus can be summarized as in Table 4.

Table 4 Beam element library in ABAQUS (Abaqus 6.11 doc)

| Beam in space | Beam theory | Node definition | Active DOF | Nodal coordinate required | Element property definition |
|---------------|----------------------|---|---------------|--|--|
| B31 | Timoshenko beam | 2-node beam linear | 1,2,3,4,5,6 | Beams in space: X, Y, Z , also (optional): N_x, N_y, N_z , the direction cosines of the second local cross-section axis. | The orientation of the local beam section axes in space is defined in terms of a local, right-handed axis system, and can be user-defined or calculated by Abaqus. |
| B31H | Timoshenko beam | 2-node beam linear, hybrid formulation | 1,2,3,4,5,6 | | |
| B33 | Euler-Bernoulli beam | 2-node cubic beam | 1,2,3,4,5,6 | | |
| B33H | Euler-Bernoulli beam | 2-node cubic beam, hybrid formulation | 1,2,3,4,5,6 | | Use only the arbitrary, I, L, and linear generalized section types |
| B31OS | Timoshenko beam | 2-node linear open section beam | 1,2,3,4,5,6,7 | | |
| B31OSH | Timoshenko beam | 2-node linear open section beam, hybrid formulation | 1,2,3,4,5,6,7 | | |

Euler-Bernoulli beams in ABAQUS do not allow for transverse shear deformation; plane sections initially normal to the beam's axis remain plane (if there is no warping) and normal to the beam axis. They should be used only to model slender beams. For beams made of uniform material, typical slenderness ratio should be less than about 1/15 (slenderness ratio is the ratio of cross-section dimension to typical axial distance). These cubic beam elements are written for small-strain, large-rotation analysis (Abaqus 6.11 doc, Section 28.3.3).

Timoshenko beams allow for transverse shear deformation. They can be used for thick (“stout”) as well as slender beams. For beams made from uniform material, shear flexible beam theory can provide useful results for cross-sectional dimensions up to 1/8 of typical axial distances or the wavelength of the highest natural mode that contributes significantly to the response (Abaqus 6.11 doc, Section 28.3.3).

ABAQUS assumes that the transverse shear behavior of Timoshenko beams is linear elastic with a fixed modulus, so that independent of the response of the beam section to axial stretch and bending (Abaqus 6.11 doc, Section 28.3.3).

Beam element formula

Abaqus 6.11 theory manual (section 3.5.2) describes that for a given stage in the deformation history of beam the position of a material point in the cross-section is given by the expression:

$$\hat{x}(S, S^\alpha) = x(S) + f(S)S^\alpha n_\alpha(S) + w(S)\psi(S^\alpha)t(S) \quad (3.10)$$

$x(S)$ is the position of a point on the centerline, $n_\alpha(S)$ are unit orthogonal direction vectors in the plane of the beam section, $t(S)$ is the unit vector orthogonal to n_1 and n_2 , $\psi(S^\alpha)$ is the warping function of the section, $W(S)$ is the warping amplitude, and $f(S)$ is a cross-sectional scaling factor depending on the stretch of the beam. S define functions of the beam axis coordinate and the cross-sectional coordinates represented by S^α , which are assumed to be distances measured in the original (reference) configuration of the beam. The warping function is chosen such that the value at the origin of the section vanishes: $\psi(0) = 0$

It is assumed that at the integration points along the beam, the beam section directions are approximately orthogonal to the beam axis tangent s given by

$$s = \lambda^{-1} \frac{dx}{dS} \quad (3.11)$$

where λ is the axial stretch given by

$$\lambda = \frac{dx}{dS} \quad (3.12)$$

The normal condition is enforced numerically by penalizing the transverse shear strains

$$\gamma_\alpha = s \cdot n_\alpha \quad (3.13)$$

This condition is assumed to be satisfied exactly in the original configuration. In what follows, ϵ_α^β is the alternator:

$$\epsilon_1^2 = -\epsilon_2^1 = 1, \epsilon_2^2 = 0 \quad (3.14)$$

The curvature of the beam is defined by

$$b_\alpha = \epsilon_\alpha^\beta t \cdot \frac{dn_\beta}{dS} \quad (3.15)$$

The ‘‘bicurvature’’ of the beam is defined by

$$X = \frac{dw}{dS} \quad (3.16)$$

The bicurvature defines the axial strain variation in the section due to the twist of the beam. Circular beam section has no warping.

CHAPTER 4

APPLIED FORCE

4.1 Uniform Load

Figure 19 shows uniform load distributed over the length of the flexible beam structure.

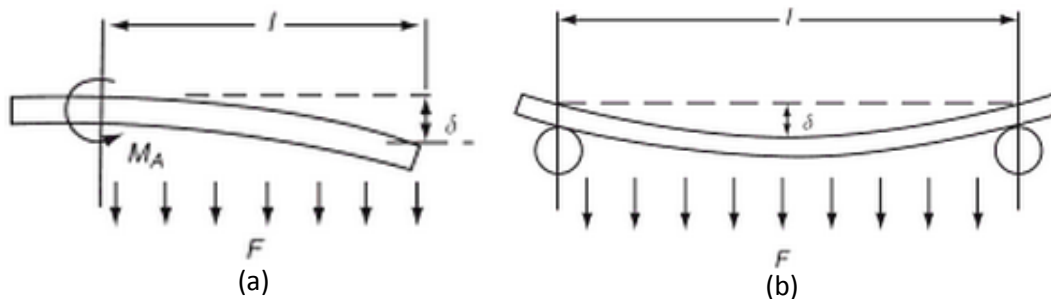


Figure 19 Uniform load on the flexible beam structure: (a) with free-end, (b) jointed-both end
(Ashby and Jones, 2012)

The relation between acting force and its deflection can be described as follows:

$$\delta = \frac{1}{8} \left(\frac{Fl^3}{EI} \right) \quad (4.1)$$

$$M_A = Fl \quad (4.2)$$

Eq. (4.1) and (4.2) are the displacement δ and bending moment M of beam structure in Figure 19 (a). Where F is the applied force and l , E , I , are the length of the beam, modulus elasticity, and second moment of inertia, respectively.

$$\delta = \frac{1}{384} \left(\frac{Fl^3}{EI} \right) \quad (4.3)$$

For beam structure with join in both ends (Figure 19 b) the deflection is represented by the equation (4.3) and maximum moment is $\frac{Fl}{8}$ at mid span.

In static loading the loads are applied not varying with time. Dynamic loads, damping, and inertia effect are neglected (Steffen, 2012).

In ABAQUS distributed loads can be model as distributed line loads which can be applied to beam elements as element-based distributed loads (Table 5). The units of a line load are force per unit length. Line load can be specified on beam elements in the global X-, Y-, or Z-direction or on beam elements in the beam local 1- or 2-direction (Abaqus 6.11 doc, Section 32.4.3). Load magnitudes in general analysis must always be given as total values, not as changes in magnitude (Abaqus 6.11 doc, Section 32.4.1).

Table 5 Load region

| Load type | Load definition | Input file region | Abaqus/CAE region |
|---------------------------|-----------------|------------------------------|---|
| Edge loads and line loads | Element-based | Element edges | Surface defined as collection of geometric edge or element edge |
| | Surface-based | Geometric edge-based surface | |

CHAPTER 5

SINTEF EXPERIMENT

5.1 Description

Experiment study needs to be done in order to have enough understanding about structural response of net panel due to uniform current as applied load.

SINTEF Fisheries and Aquaculture conducted an experiment of net panels with different bending stiffness, results that were compared with a model in FhSim (Gansel et al., 2013). The experiment was focus on the deformation of nets normal to uniform currents and conducted in the North Sea Center flume tank in Denmark. Related to deformation of the net panel, PET net with bending stiffness was clamped between two steel bars as shown in Figure 20 and net was quadratic with a side length of 1m.

The tests were run without a stiff metal rod mounted in the lower edge of the nets, so that unsuppressed the deformations in the y-direction during the tests. To determine the deflection of the net a Qualisys motion tracking system was used, the Qualisys system determine the 3-dimensional positions of reflective spheres mounted on the steel bar, the metal rod and different locations on the nets. A velocity meter was mounted 3000 mm upstream from the nets with an offset of 800 mm from the center of the frame in y-direction. The nets were tested at 6 different flow speeds (0 m/s, 0.13 m/s, 0.25 m/s, 0.38 m/s, 0.5 m/s and 0.63 m/s).

In Figure 20, view to the right, it can be seen the net panels clamped in between rigid metal bars, the red circles in the image indicate the positions of reflective markers used to control the 3-dimensional orientation of the frame using a Qualisys motion tracking system. In the drawings to the left, the metal bars are red, the multi-axis force/torque measurement system is green and the velocity meter is yellow (Gansel et al., 2013).

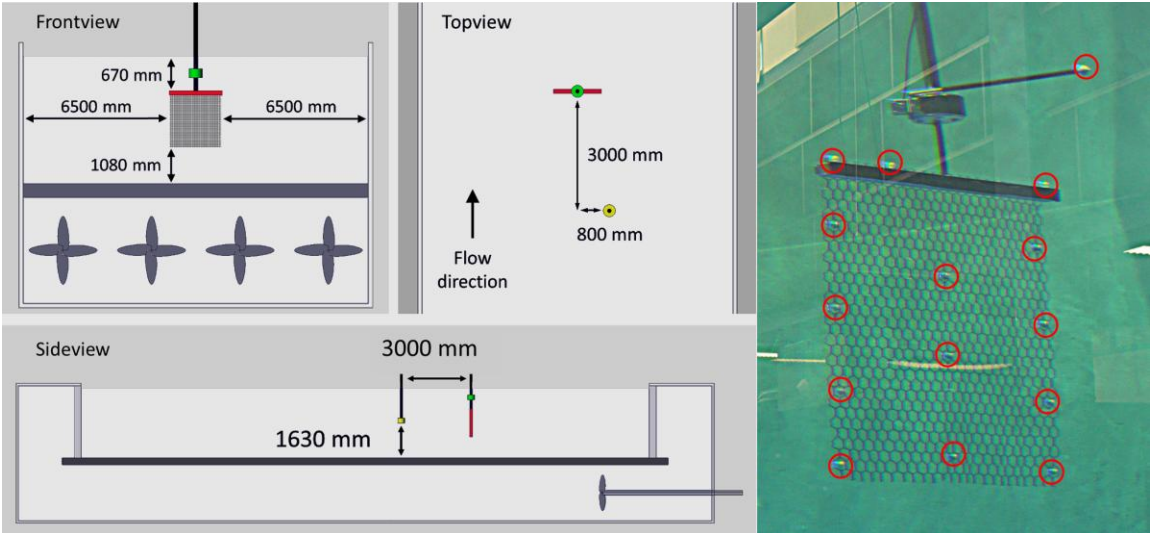


Figure 20 Set-up of the experiments (Gansel et al., 2013)

5.2 Experiment Data

It is important that to mention that all the required data are available before start the modeling in ABAQUS. Geometry, dimension and material properties of PET net are needed for modeling of net structure in ABAQUS (Figure 21, Table 6 and Table 7). For each flow speed, drag forces with its coordinate on the net panel that were measured during the experiment is collected as the applied loads that act on the net panel. The complete result of the experiment is also documented for the deformation comparison between model in the experiment and model from ABAQUS. This result can be seen in more detail in Chapter 7.

Table 6 Specification and dimension of PET net (Gansel et al., 2012)

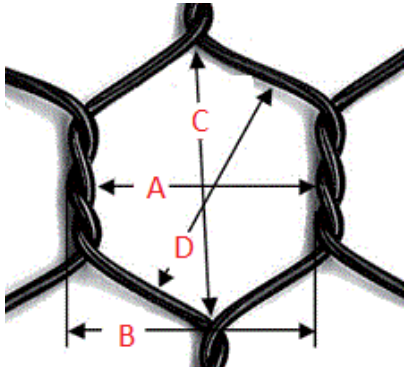


Figure 21 Geometry of PET net

| | |
|--|-----------|
| Solidity | 0.14 |
| Twine Diameter (cm) | 0.25 |
| Half mesh size (cm) | NA |
| Aperture form | Hexagonal |
| R _n -range (approx.) [10 ³] | 1-2.2 |
| A (cm) | 3.5 |
| B (cm) | 4.0 |
| C (cm) | 4.3 |
| D (cm) | 3.7 |

Table 7 Material properties of PET net (Designerdata)

| | |
|---|-----------|
| Density (g/cm^3) | 1.3-1.4 |
| Young's modulus of elasticity (10^9 N/m^2) | 2.8-3.1 |
| Shear modulus (10^9 N/m^2) | 0.7-2 |
| Ultimate tensile strength (10^6 N/m^2) | 55 |
| Poisson's ratio | 0.37-0.44 |

5.3 Result

Considering that the comparison in this thesis has been done with the PET net panel, here it will be briefly present the results from the experiments corresponding to that material.

The results for the deformation of the PET net can be seen in Figure 22 and Table 8 which shows the average positions of markers mounted on net panels in the x-z plane with varying current speed.

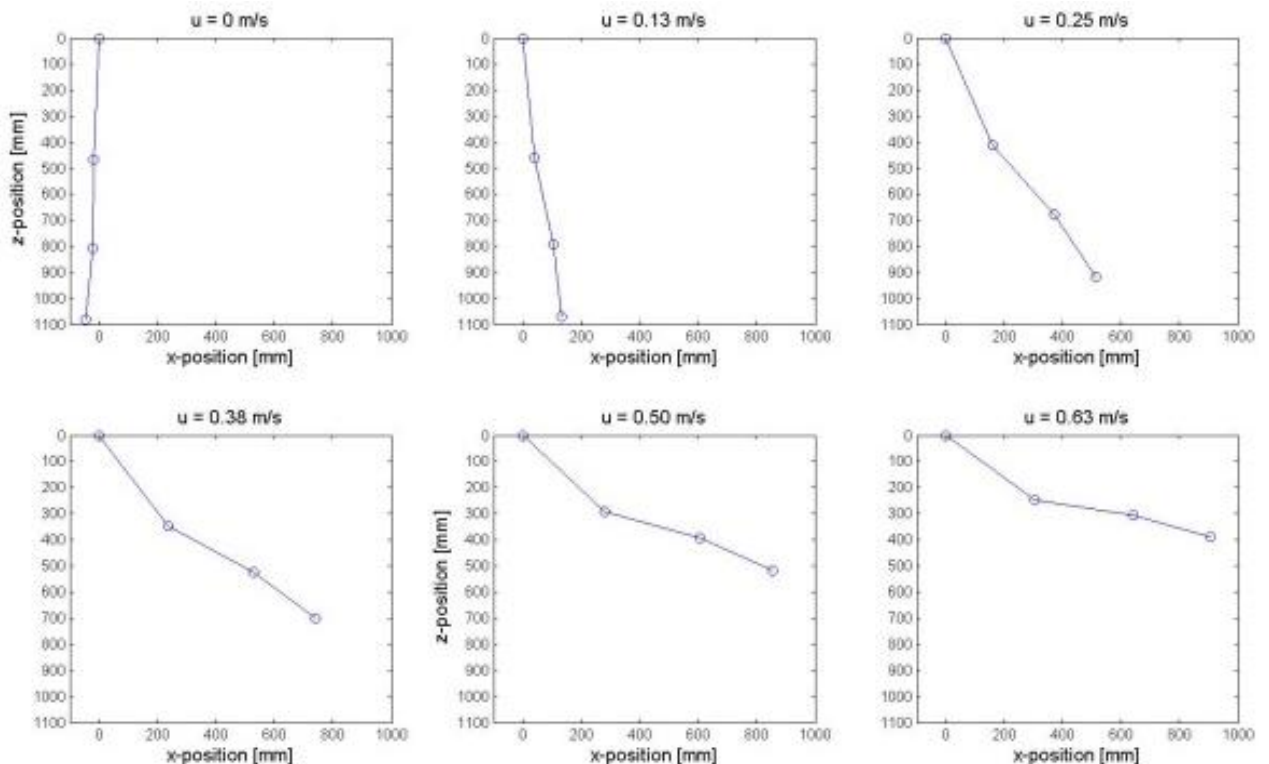


Figure 22 Deformation of PET net in the x-direction at different flow speeds (Gansel et al., 2013)

Table 8 Drag forces and its coordinate

| Flow speed [m/s] | Drag force [N] | Position | | | | | | | |
|------------------|----------------|----------|--------|--------|--------|--------|--------|--------|--------|
| | | x [P1] | x [P2] | x [P3] | x [P4] | z [P1] | z [P2] | z [P3] | z [P4] |
| 0 | 0.135 | 0 | -0.019 | -0.021 | -0.047 | 0 | 0.465 | 0.806 | 1.081 |
| 0.13 | 2.631 | 0 | 0.041 | 0.105 | 0.132 | 0 | 0.458 | 0.793 | 1.069 |
| 0.25 | 6.922 | 0 | 0.161 | 0.373 | 0.513 | 0 | 0.411 | 0.678 | 0.917 |
| 0.38 | 11.896 | 0 | 0.236 | 0.530 | 0.741 | 0 | 0.349 | 0.523 | 0.702 |
| 0.5 | 17.992 | 0 | 0.280 | 0.606 | 0.855 | 0 | 0.292 | 0.394 | 0.518 |
| 0.63 | 25.636 | 0 | 0.305 | 0.642 | 0.907 | 0 | 0.248 | 0.305 | 0.391 |

From Table 8 it is important to notice that the initial position in the experiment the PET net panel has an initial deformation when no load is apply. Additionally, it has been possible to calculate the distance between the initial and final position of the sensors corresponding to the different flow speed (Table 9), these in order to compare experimental and ABAQUS results.

Table 9 Distance displacement at each position

| Flow speed [m/s] | Position 1 | Position 2 | Position 3 | position 4 |
|------------------|------------|------------|------------|------------|
| 0.13 | 0 | 0.0603 | 0.1272 | 0.1792 |
| 0.25 | 0 | 0.1879 | 0.4144 | 0.5830 |
| 0.38 | 0 | 0.2808 | 0.6193 | 0.8749 |
| 0.5 | 0 | 0.3457 | 0.7507 | 1.0635 |
| 0.63 | 0 | 0.3905 | 0.8313 | 1.1776 |

CHAPTER 6

MODELING

6.1 Methodology Overview

The general methodology overview can be seen in Figure 23. The work begins with the study of SINTEF experiment in order to have enough understanding and knowledge about the detailed setting of PET net panel experiment such as: the net panel structure, applied force, response of the net panel, and final result. All of required data from SINTEF experiment need also to be collected before start the modeling in ABAQUS. Detail of SINTEF experiment with its data and result has been described in Chapter 5.

In order to obtain an accurate model in ABAQUS the user should have good capability to operate it regarding to design and requirements of the model. The knowledge about modules application in ABAQUS and its finite element theories is also important for the user to construct PET net model. The twist section are also challenging for the ABAQUS user because it is quite difficult to assign its motion when is subjected to the loads. In Chapter 3, further details of the modules, beam element, and load in ABAQUS were briefly described.

From the available data, modeling of net panel structure can be done. During the modeling process, the ABAQUS user should ensure that model has correct geometry, material properties, boundary condition and constraint to represent given degree of freedom, proper meshing, and applied hydrodynamic loads. The modeling will be finished if is able to represent the general behavior of the structure, otherwise the step need to return to modeling process. The complete steps in modeling PET net panel in ABAQUS are explained further in this chapter.

The result from ABAQUS will be analyzed after the modeling is finished (Chapter 7). The following points need to be fulfilled to ensure that the model has been created under the correct design criteria:

- 1) Applied force is in equilibrium with reaction force,
- 2) Used boundary conditions is able to represent the motion of vertical section
- 3) Displacement output from each velocity are comparable with experiment result

The output from modeling in ABAQUS will be compared with the result from experiment. The displacement in its given coordinate from the experiment will be plotted together with displacement output in ABAQUS. Further discussion about the response of model in ABAQUS in different velocities compare to experiment result is in Chapter 8.

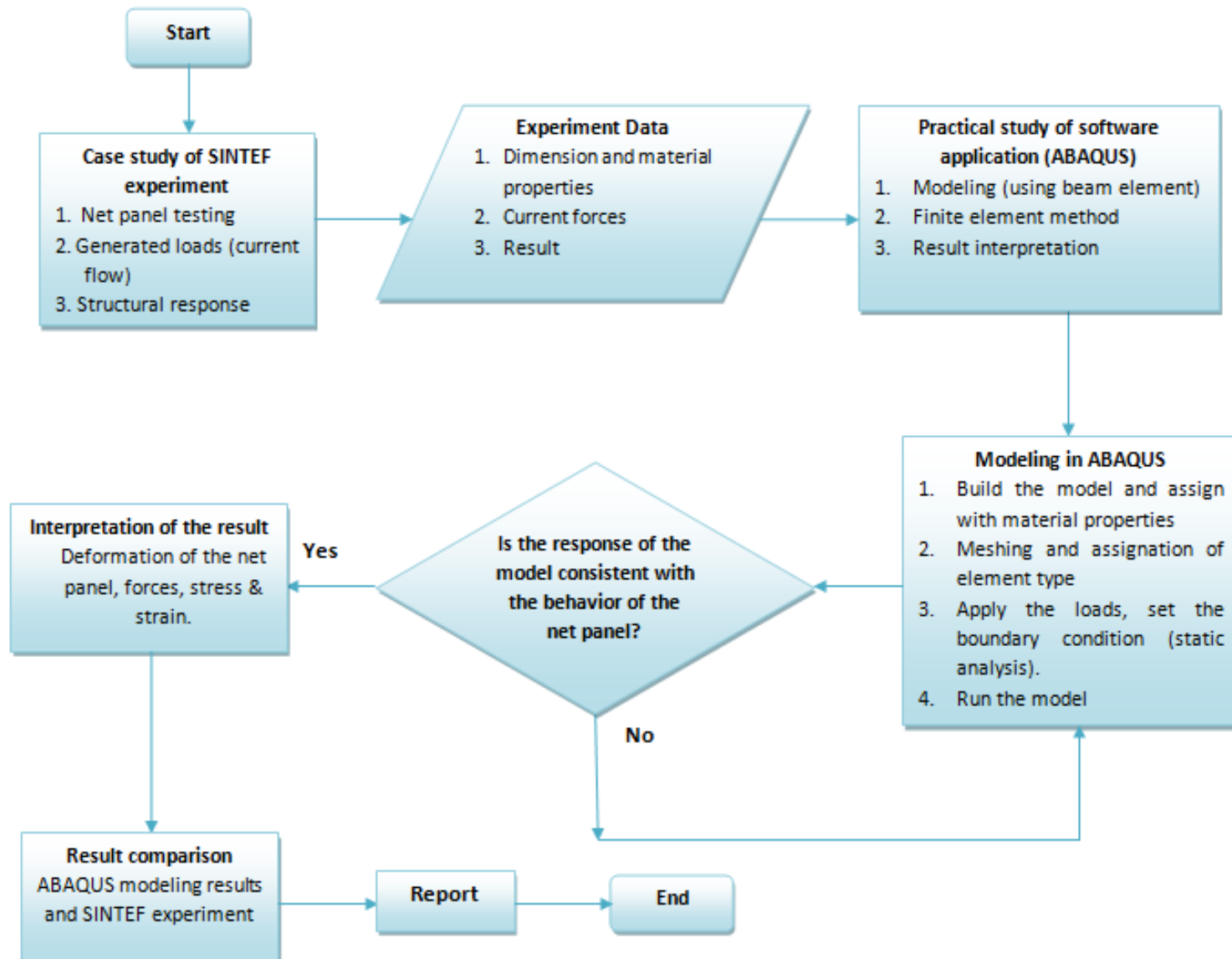


Figure 23 Methodology flow chart

6.2 Net Panel Modeling

As mentioned before one of the objectives of this thesis is to model the PET net panel in ABAQUS according to the PET net specifications used in SINTEF experiment. Hence, in each of the following modules the structural modeling process will be explained in more detail.

Part

The net panel model was built as one part using 3D deformable wire. The part consists of a mesh structure (Figure 24), 15 in length and 25 in width to model 1 m x 1 m PET net panel. Each mesh is constructed in hexagonal shape. The dimension of each mesh corresponds as the one used by SINTEF in the experiment (Table 6).

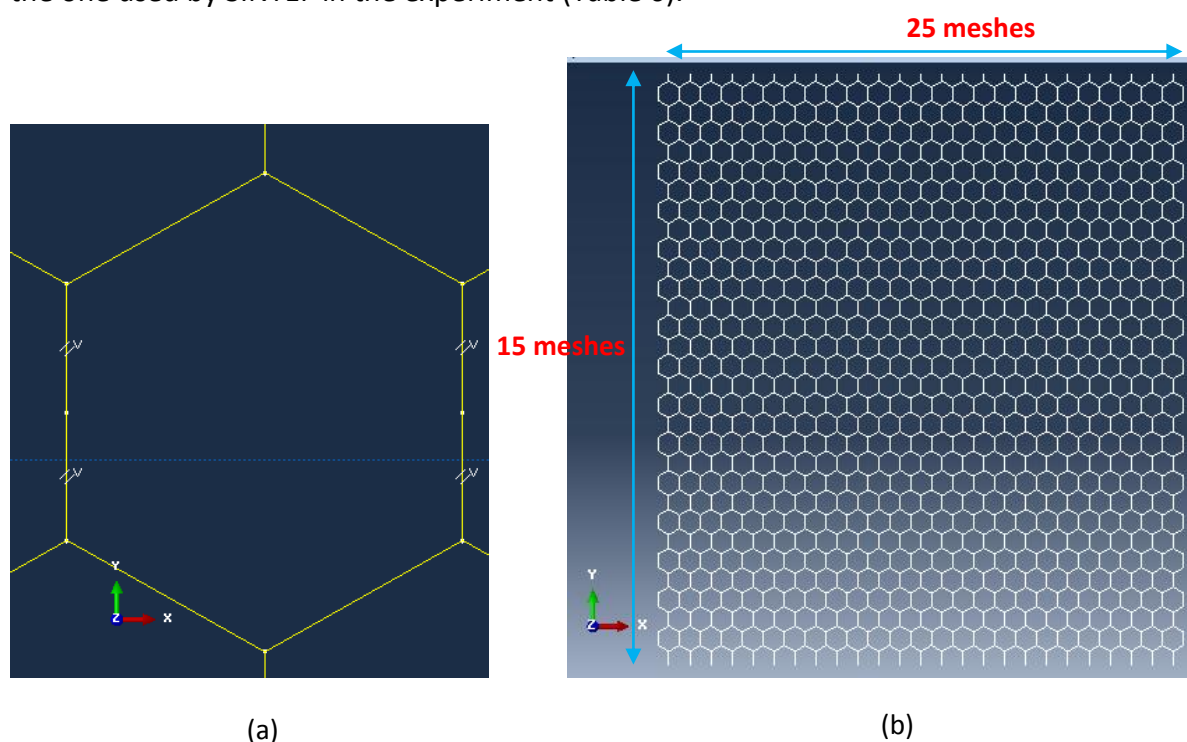


Figure 24 (a) Hexagonal shapes of a mesh and (b) PET net panel visualization in Part module

Property

In this module the section and the type of material with its properties are assigned. The material properties of PET that have been used for modeling were according to the material properties (Table 7);

Density = 1380 Kg/m^3

Young's modulus (E) = 3000 MPa

Poisson's ratio = 0.39

Shear modulus (G) = 2000 Mpa

The beam profile was designed to have circular profile and each mesh of the net panel was built using two different diameters, vertical and diagonal profile with diameter 0.0025m and

0.00125m, respectively. It was decided to use a bigger diameter for the vertical bar, which corresponds to the outer part of the two twisted bars, in order to simplify the twisted vertical bar of the PET net (Figure 21), in Figure 25 it is shown the diagonal and vertical section of the net panel modeled in ABAQUS.

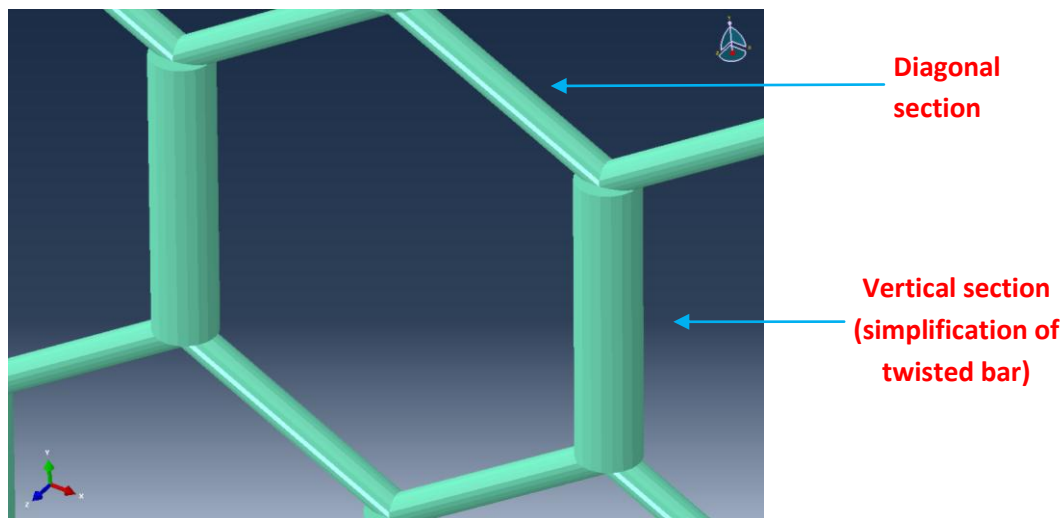


Figure 25 Diagonal and vertical section on a mesh with circular beam profile

Mesh

Dependent part instance was used in this modeling. Hence, the meshing is defined on the original part and applied the same to all instance of the part. The meshing result can be seen in Figure 26. The following values were specified into the modeling:

- Seed size : 0.01
- Element type : B31

Giving as a result from the meshing:

Number of nodes = 3845

Number of elements = 4555

After meshing, there are two elements in each vertical and diagonal section of net panel and each element has two nodes. Timoshenko beam element (B31) is used to take into account the bending and shear deformation.

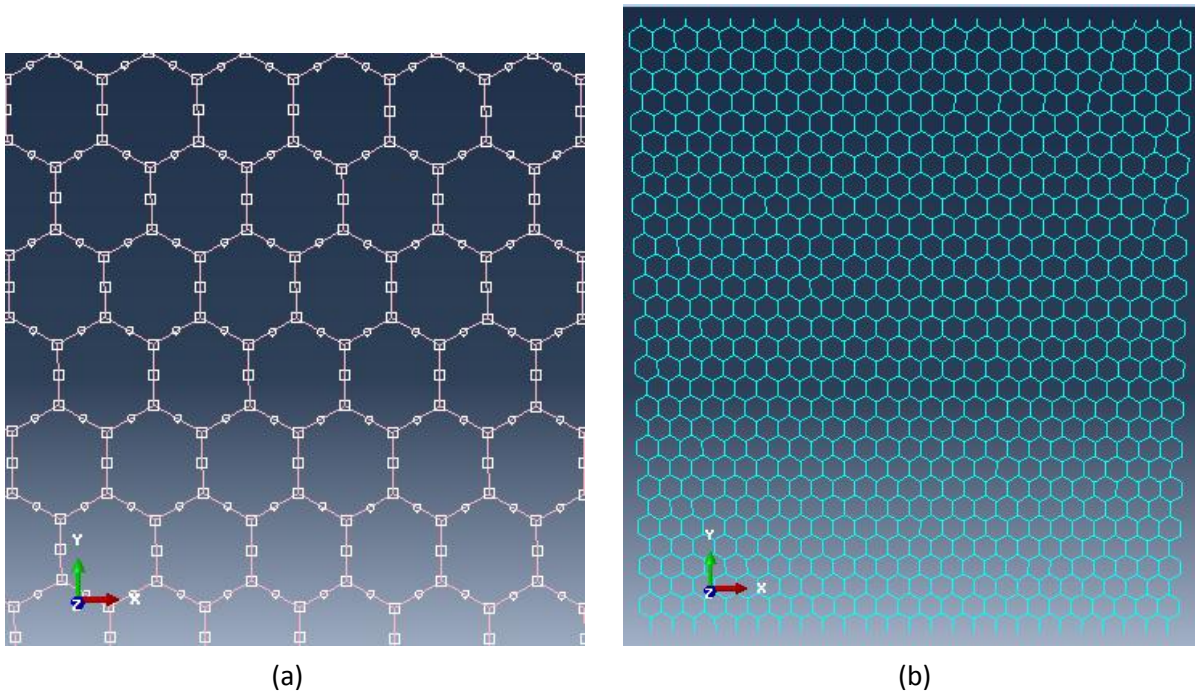


Figure 26 (a) Seed with 0.01 m in size and (b) the model visualization after meshing (right)

Step

The type of step was static general with a time period of 2 second, having 100 as a maximum number of increments and applying the load linearly over the step. In this modeling a static analysis has been used considering that the forces acting on the net panel are unchanged in time (steady current) and also neglecting inertia effects. The boundary conditions and load definition that has been assigned before contributed during the step to determine the result in elements and nodes output (Figure 27).

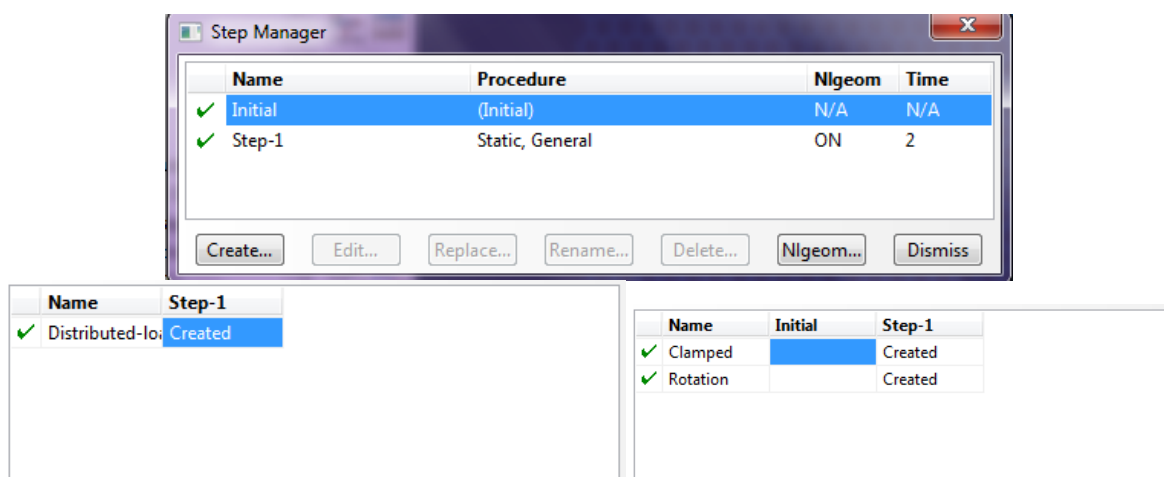


Figure 27 Static general steps

Load

As mentioned in Chapter 5, the current force in the experiment is acting perpendicular to the net panel. Thus in this modeling, the type of load was a distributed line load applied over the whole net panel with direction to the $-z$ direction (Figure 28) or perpendicular to the element. As a result, this drag force of current is assumed as static load where the total drag forces from each current velocity were divided by the total length of all elements on the net panel (Table 10) to obtain force per unit length. Therefore, line load is expected can represent the uniform distributed current acting over the net panel. The length of diagonal and vertical elements are; 0.02039 m and 0.023m, respectively.

Table 10 Force per unit length calculation

| Drag force [N] | Number of element | | Total length of all elements [m] | Drag force per unit length [N/m] |
|-------------------|-------------------|----------|---|--|
| | Diagonal | Vertical | | |
| 2.6310 | 1500 | 765 | 48.18 | 0.0546 |
| 6.9224 | | | | 0.1437 |
| 11.8964 | | | | 0.2469 |
| 17.9918 | | | | 0.3734 |
| 25.6363 | | | | 0.5321 |

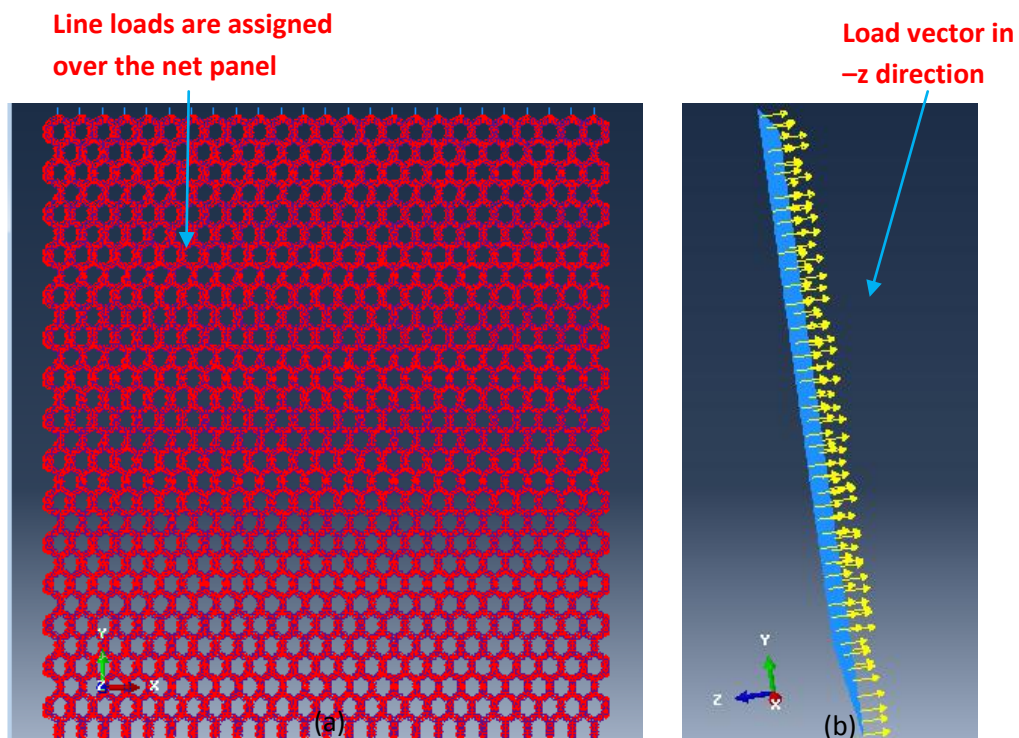


Figure 28 (a) Region of applied loads and (b) load direction

Boundary conditions

The boundary conditions applied in the model were set as follows:

- 1) Clamped at the top restricting any translation or rotation in the upper nodes
- 2) The boundary condition in the nodes on the vertical section allows the rotation around the y-axis (vertical direction) and gives stiffness for the DOF in the vertical bar.

Figure 29 and Figure 30 show the boundary conditions used for the modeling. The clamped boundary condition represents the clamp on the net panel in the experiment, and the boundary condition of the nodes in the vertical bar simulates the motion of the twist bar on the PET net in translation and rotation. The translation degree of freedom in the x-direction and the rotation degree of freedom around z-direction were constrained to give stiffness in the vertical bar “twisted form” (Figure 30 b).

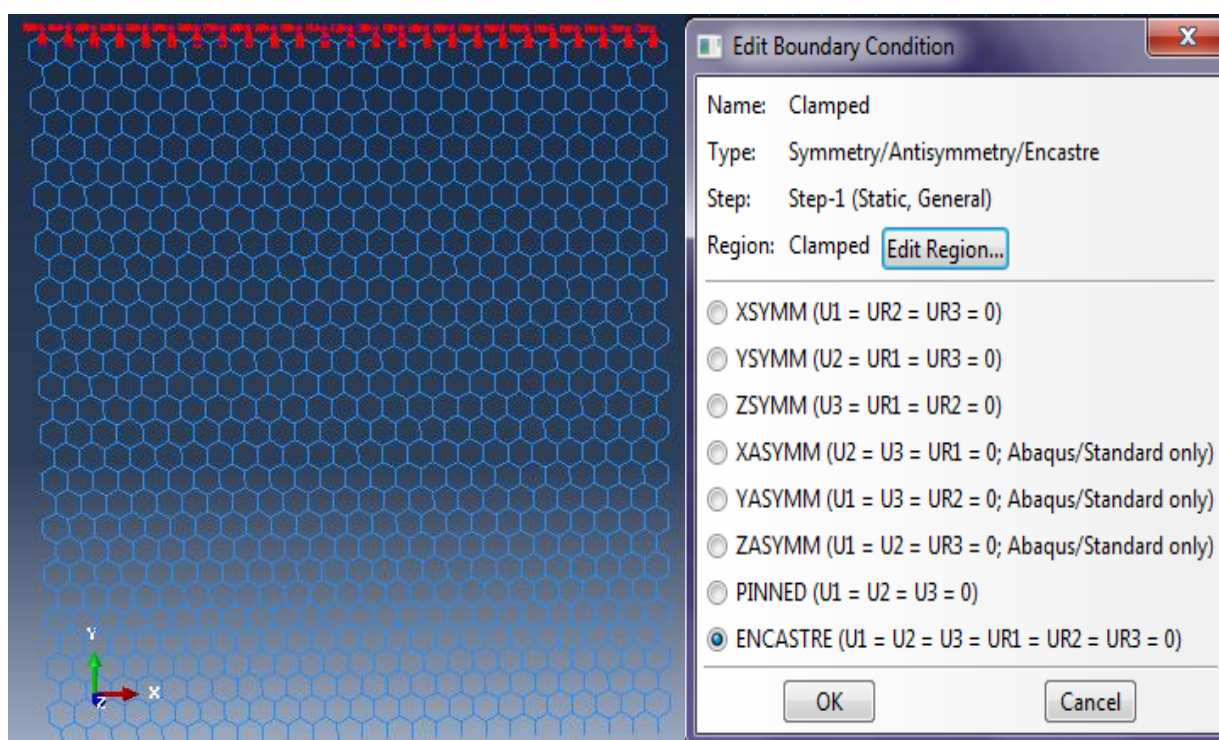
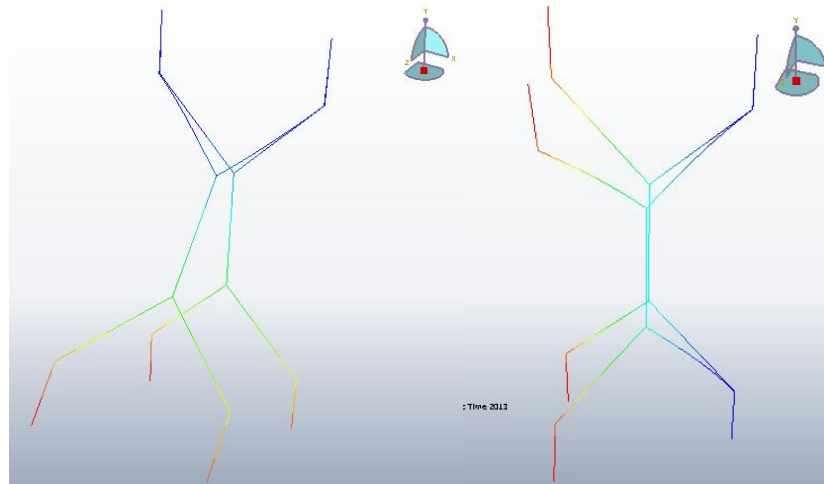
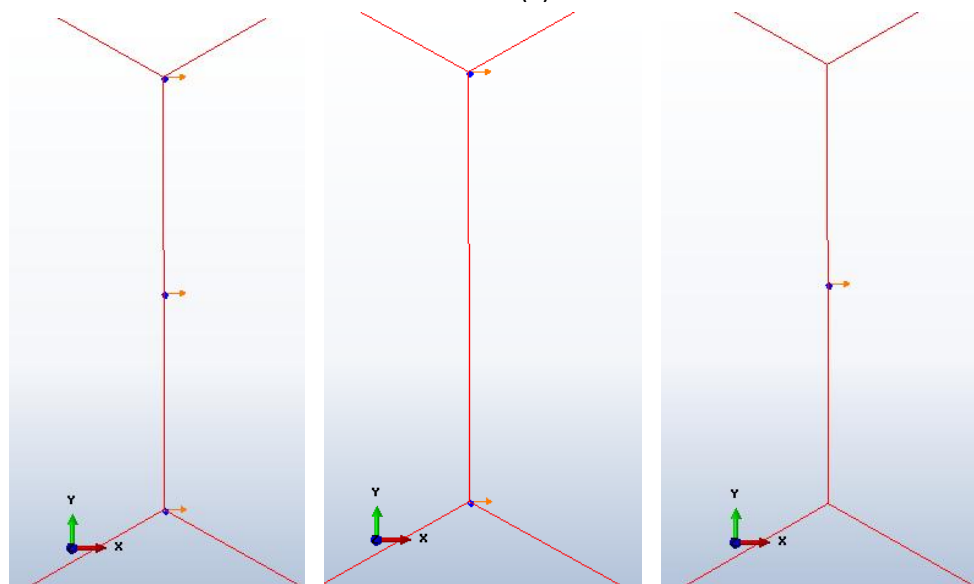


Figure 29 Clamped boundary conditions



(a)



(b1)

(b2)

(b3)

Figure 30 (a) Rotation and translation in vertical bar (b) Boundary conditions in the three nodes of the vertical bar: (b1) Case 1, (b2) Case 2, (b3) Case 3

Considering the simplification of the vertical bar and in order to obtain the right amount of stiffness, the vertical bar was built with three nodes and applying different cases of boundary conditions. Thus the modeling was run in three cases in order to see the best fit case to the experiment results (Table 11).

Table 11 Modeling cases

| | |
|---------------|---|
| Case 1 | Rotation in 3 nodes from the vertical bar |
| Case 2 | Rotation in 2 nodes and the middle following the movement |
| Case 3 | Rotation in middle node while the others two follows the movement |

CHAPTER 7

MODELING RESULTS

7.1 Validation of model

Forces

According to the theoretical background from Finite Element Method (Chapter 3) it is necessary to check if the applied load corresponds to the reaction force, in that way it is possible to be sure that there is equilibrium of forces in the model. Thus in Table 12 are presented all the applied loads with their respective reaction force, from there it can be seen that the force applied, same as the force from the experiment, corresponds to the reaction force from ABAQUS at each load.

Table 12 Experimental forces from SINTEF experiment and reaction forces from ABAQUS results at different flow speed

| Flow Speed [m/s] | Experiment Force [N] | Reaction Force [N] | | |
|------------------|----------------------|--------------------|---------|---------|
| | | Minimum | Maximum | Total |
| 0.13 | 2.6310 | -1.3221 | 11.3468 | 2.6318 |
| 0.25 | 6.9224 | -3.1057 | 4.0156 | 6.9250 |
| 0.38 | 11.8964 | -2.9328 | 3.8043 | 11.8997 |
| 0.5 | 17.9918 | -2.7301 | 4.0516 | 17.8325 |
| 0.63 | 25.6363 | -2.3885 | 4.2556 | 25.6408 |

Strain vs. Stress

In Figure 31 is plotted the strain versus stress of the PET net panel under the maximum load (25.63 N). The plot shows that the result follows a linear elastic theory, meaning that the Young's modulus is constant in the whole analysis obeying the Hooke's law, and there is not permanent deformation of the material. In other words the analysis of the PET net panel will occur in the elastic portion of the stress strain curve of the material and the material is not exceeding its yield strength.

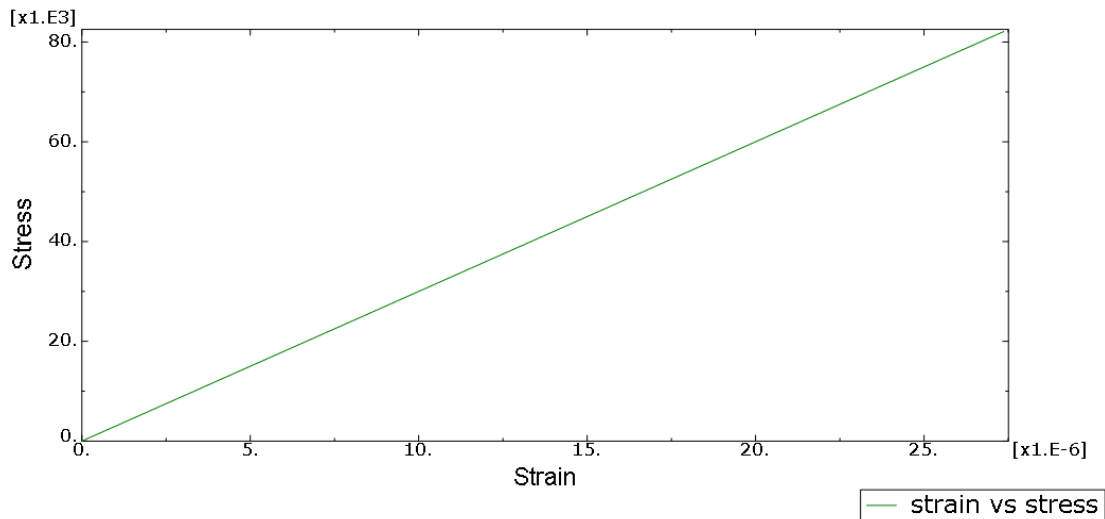


Figure 31 Stress (S_{11}) versus Strain (E_{11})

7.2 Comparison with SINTEF Experiment

As it has been explained in Chapter 5 the deflection from SINTEF experiment was estimated by taking the average position from the position sensors. For that reason and in order to compare the results from ABAQUS with the experimental results, the coordinates of the nodes similar to the sensors position in the experiment (Figure 32) were extracted. Therefore, it was possible to calculate the distance between the initial and final position (deformed) to compare them with the deflection from the experiment, outlined in Table 9.

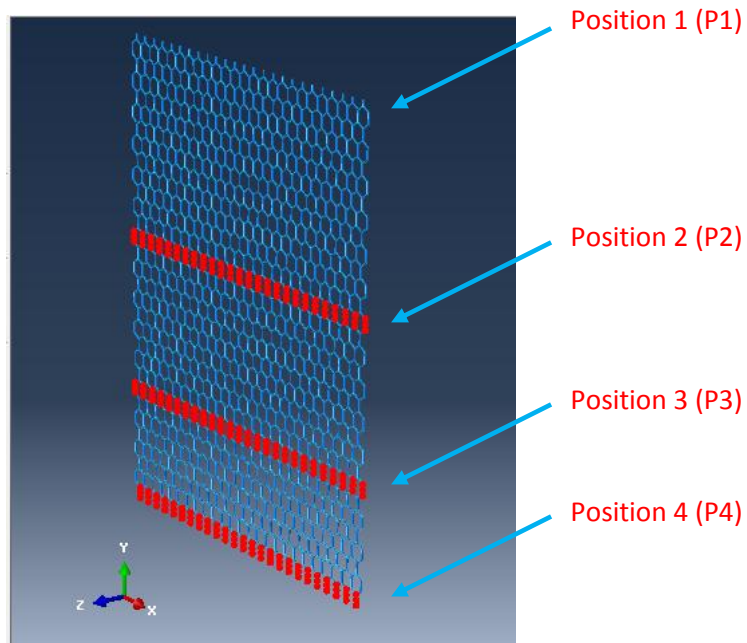


Figure 32 Nodes at the position of sensor from SINTEF experiment

As mentioned in section 6.2, the model was run in three different cases (Table 11). The results of the deflection from those cases are presented in Figure 33, Figure 34, Figure 35, Figure 36, and Figure 37 respectively.

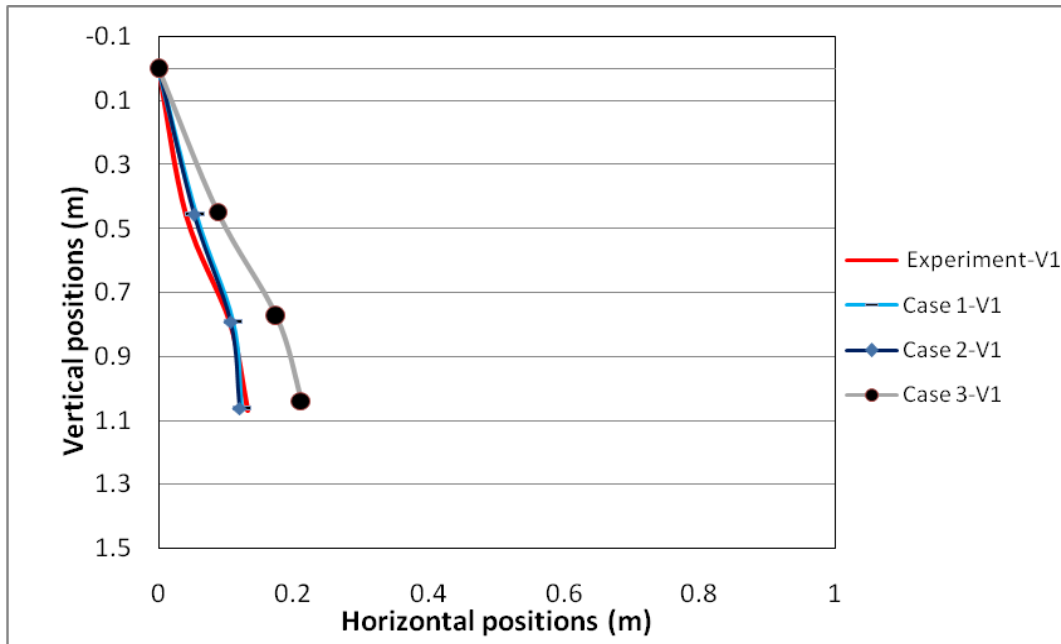


Figure 33 Comparison of deflection between cases and the experiment (V1=0.13 m/s)

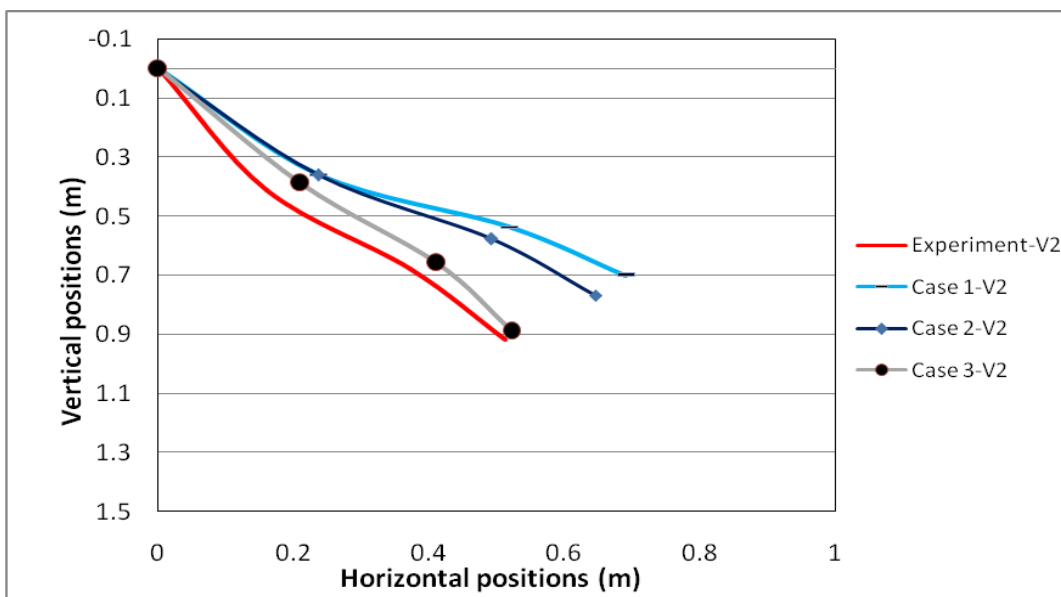


Figure 34 Comparison of deflection between cases and the experiment (V2=0.25 m/s)

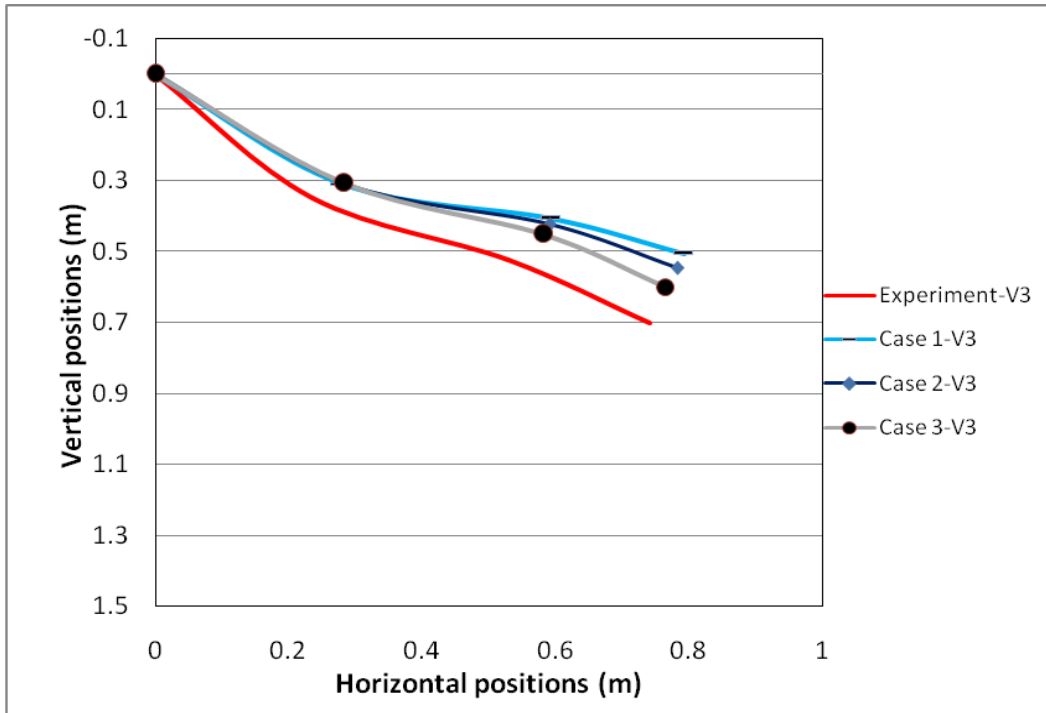


Figure 35 Comparison of deflection between cases and the experiment ($V_3=0.38$ m/s)

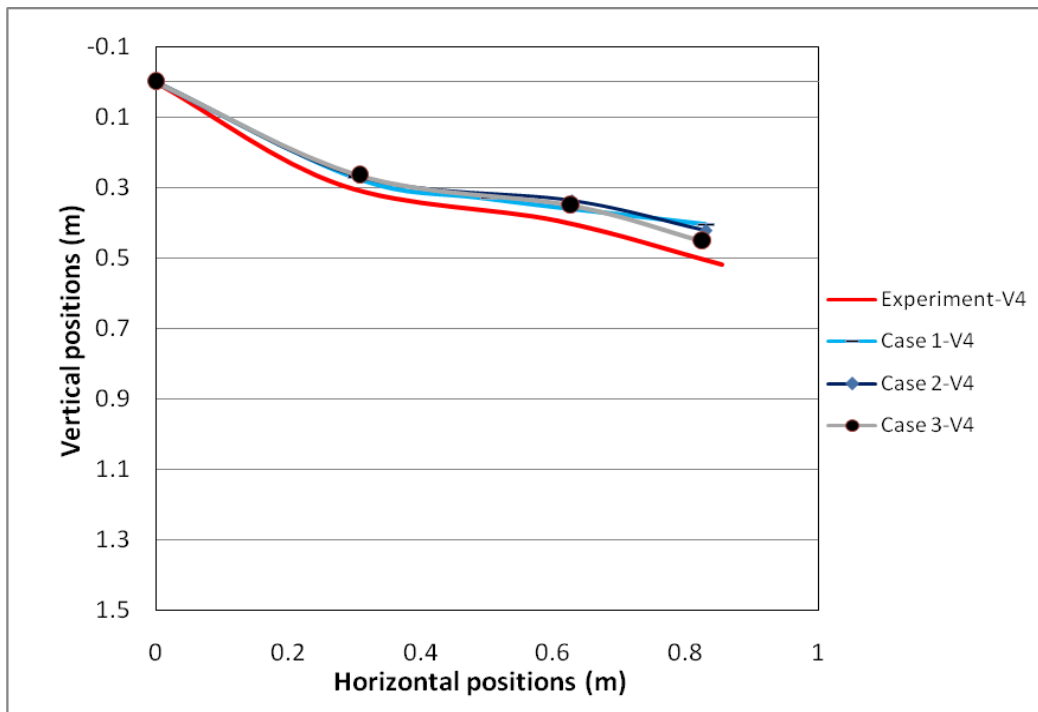


Figure 36 Comparison of deflection between cases and the experiment ($V_4=0.5$ m/s)

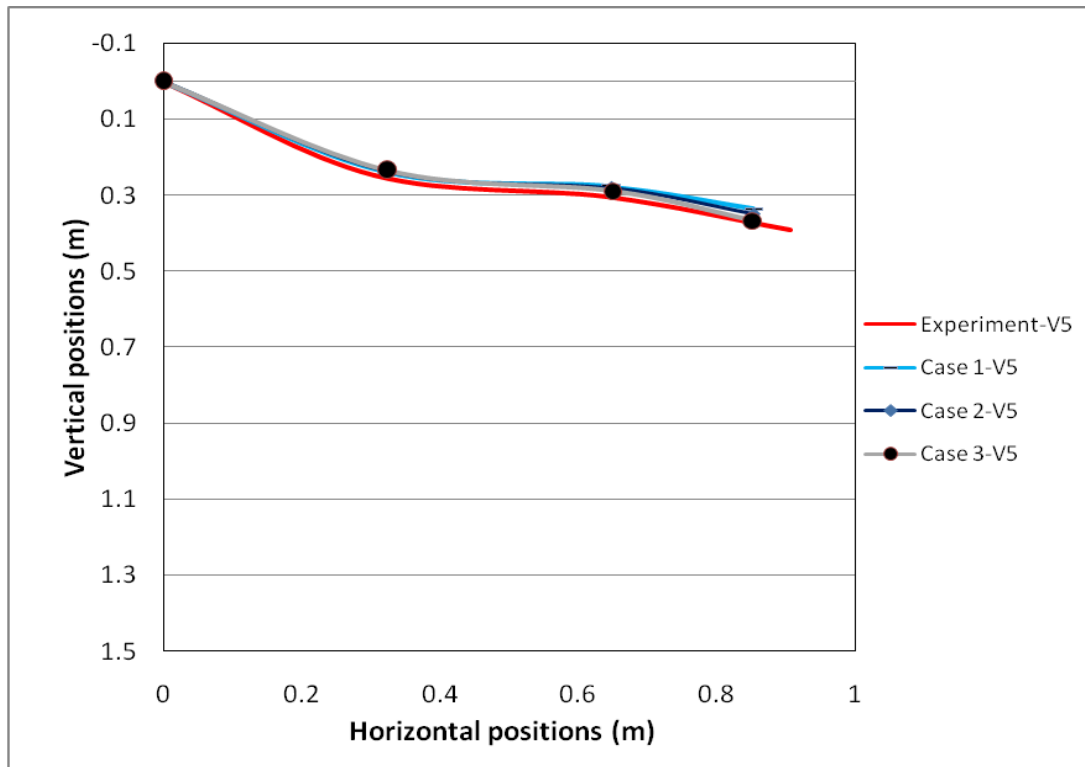


Figure 37 Comparison of deflection between cases and the experiment (V5=0.63 m/s)

In order to observe the accuracy of the different cases, Table 13 shows the displacement error of the deflection achieved from the ABAQUS results and experiment. These percentage errors were calculated by taking the difference between the distance from the experiment and the cases at each velocity for all positions. Thus it can be seen from Figure 33, Figure 34, Figure 35, Figure 36, and Figure 37 and Table 13 that case 3 gives the best solution by giving smaller percentage error (red values) for the majority of the velocities. Therefore, by modeling the interconnection bar with three nodes and by allowing the middle node to rotate (the other 2 nodes following the movement) provides the best way to structurally model the net panel.

Table 13 Percentage of displacement error

| Velocity [m/s] | Cases | Displacement error [%] | | | Average error [%] |
|----------------|-------|------------------------|-------|-------|-------------------|
| | | P2 | P3 | P4 | |
| V1 | Case1 | 0.406 | 0.135 | 0.324 | 0.289 |
| | Case2 | 0.328 | 0.073 | 0.424 | 0.275 |
| | Case3 | 1.406 | 2.117 | 2.491 | 2.005 |
| V2 | Case1 | 2.736 | 6.025 | 8.355 | 5.705 |
| | Case2 | 2.707 | 4.653 | 5.972 | 4.444 |
| | Case3 | 1.611 | 1.304 | 0.901 | 1.272 |
| V3 | Case1 | 1.711 | 3.979 | 6.024 | 3.905 |
| | Case2 | 1.846 | 3.463 | 4.788 | 3.366 |
| | Case3 | 1.871 | 2.631 | 3.117 | 2.540 |
| V4 | Case1 | 0.908 | 3.591 | 3.449 | 2.649 |
| | Case2 | 1.071 | 1.838 | 2.935 | 1.948 |
| | Case3 | 1.142 | 1.436 | 2.134 | 1.571 |
| V5 | Case1 | 0.559 | 0.842 | 2.281 | 1.227 |
| | Case2 | 0.636 | 0.743 | 2.022 | 1.134 |
| | Case3 | 0.702 | 0.537 | 1.770 | 1.003 |

In the below figure (Figure 38) is plotted the average coordinates for the different positions of the PET net panel model (case 3) and the panel from the experiment, there it can be seen that there is a better matching when the structure is under higher loads.

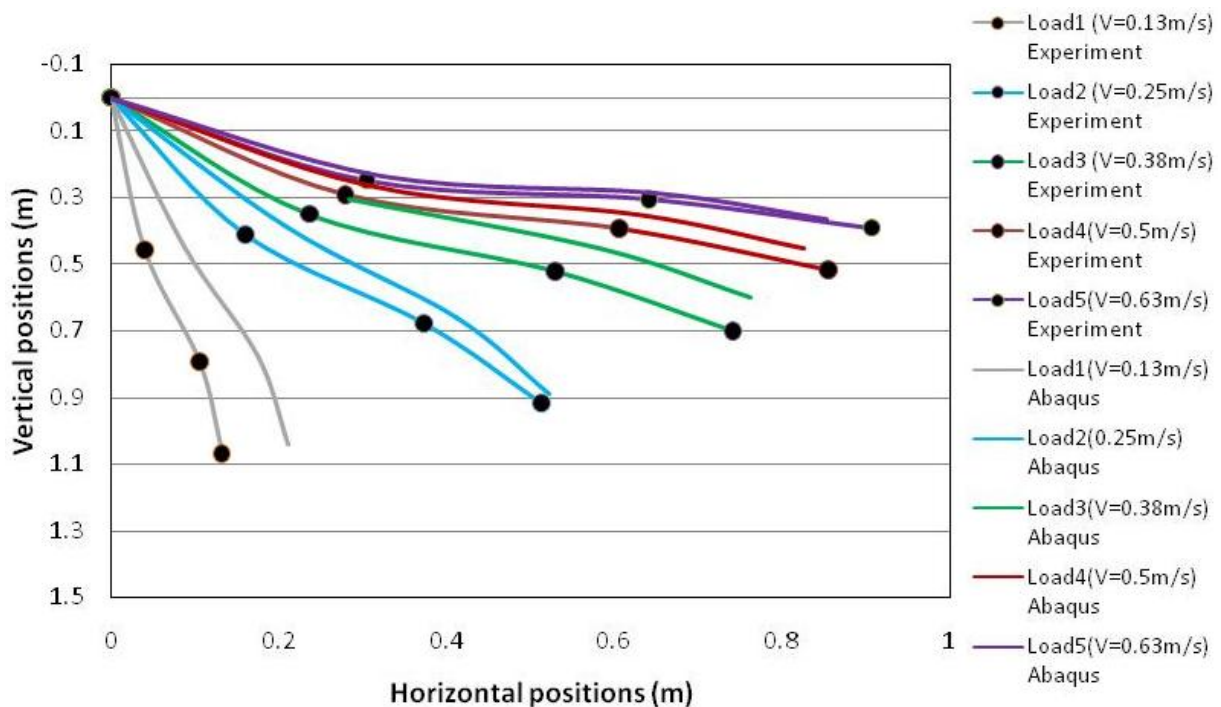


Figure 38 Average coordinates of PET net panel from ABAQUS and experiment

7.3 Displacement

Translation

The modeled net panel with case 3 type of modeling was subjected to different loadings corresponding to various current velocities as in the experiments. Note that in case of the ABAQUS loading, it was the drag force that corresponds to the current velocity that was applied. As expected the deflection is greater away from the fixed point and is greater for increasing loading conditions. Table 14 outlines the translations for different loading conditions in U1, U2 and U3 directions. As seen in the Table 14, the smallest load was 2.63 N (corresponding to the current velocity of 0.13m/s) and the largest loading was 25.6 N (corresponding to 0.63 m/s).

Generally, the displacements of all net panels are greater in U3, z-direction and increase with increasing the load. For the y-direction, U2 (vertical displacement), the values corresponds to the horizontal translation by giving larger vertical displacements for larger horizontal translations. As expected there is not deflection in the x-direction, U1, as there is no load applied in this direction.

Table 14 Average translation displacement for the different positions and under different loads.

| Position | Translational displacement [m] | Forces [N] | | | | |
|----------|--------------------------------|------------|--------|--------|--------|--------|
| | | 2.631 | 6.922 | 11.896 | 17.992 | 25.636 |
| 2 | U1 | 0.000 | 0.000 | 0.000 | 0.000 | 0.000 |
| | U2 | 0.017 | 0.077 | 0.159 | 0.200 | 0.231 |
| | U3 | -0.106 | -0.229 | -0.302 | -0.327 | -0.344 |
| 3 | U1 | 0.000 | 0.000 | 0.000 | 0.000 | 0.000 |
| | U2 | 0.032 | 0.148 | 0.354 | 0.453 | 0.505 |
| | U3 | -0.195 | -0.433 | -0.603 | -0.648 | -0.671 |
| 4 | U1 | 0.000 | 0.000 | 0.000 | 0.000 | 0.000 |
| | U2 | 0.042 | 0.193 | 0.482 | 0.623 | 0.706 |
| | U3 | -0.257 | -0.568 | -0.810 | -0.870 | -0.899 |

To visualize the results in Table 14, Figure 39, Figure 40, Figure 41, Figure 42 and Figure 43 illustrate the displacement of the PET net panel (case 3) for increasing currents speeds (note that we applied the corresponding levels of load in the ABAQUS analysis), respectively. As seen in Figure 39, Figure 40, Figure 41, Figure 42 and Figure 43, the deflection in the upper part (1/3) of the net panel is linear, while the lower part (2/3) is more like the bending deformation. This is because of the fixed boundary condition at the top and the stiffness of the material.

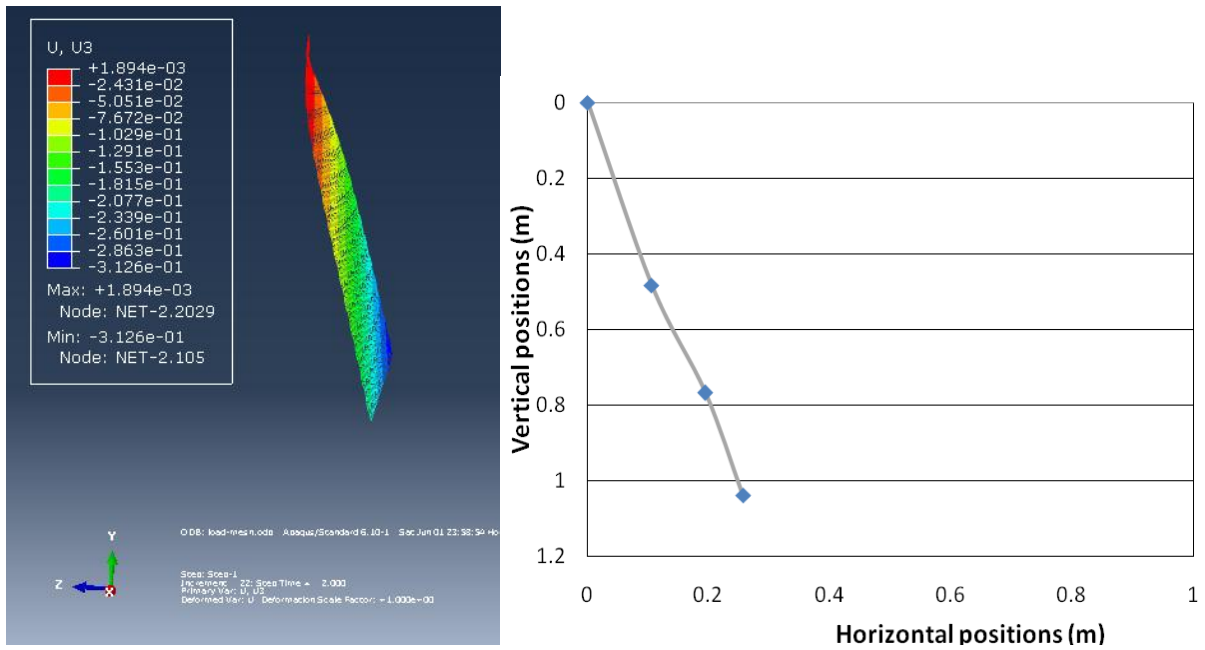


Figure 39 Deformation of model in ABAQUS (F = 2.631 N, V = 0.13 m/s)

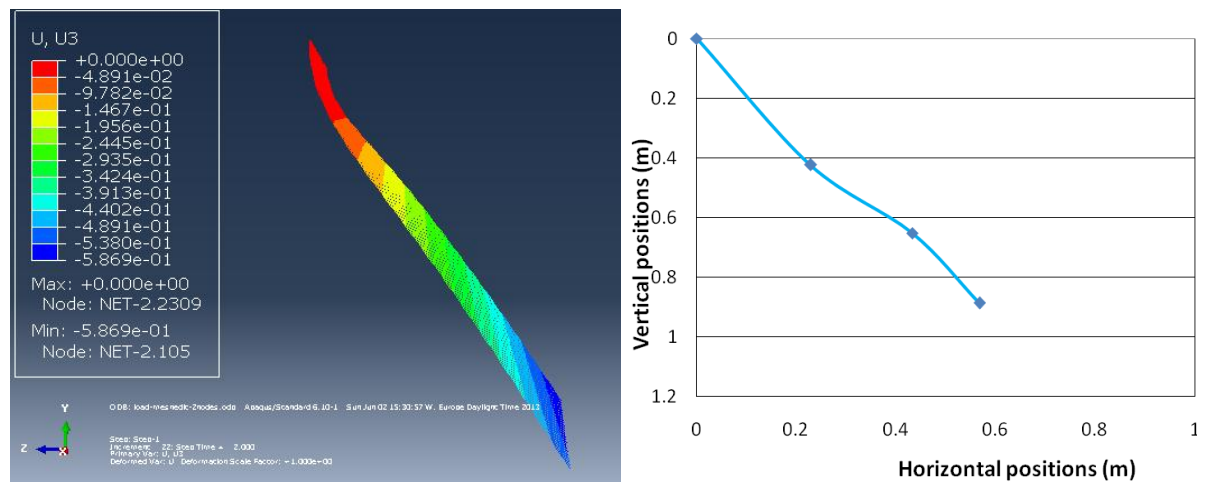


Figure 40 Deformation of model in ABAQUS (F = 6.922 N, V = 0.25 m/s)

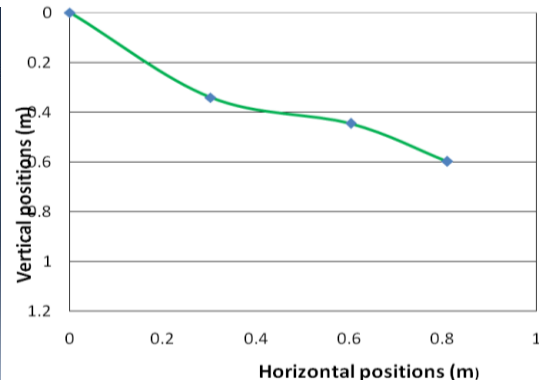
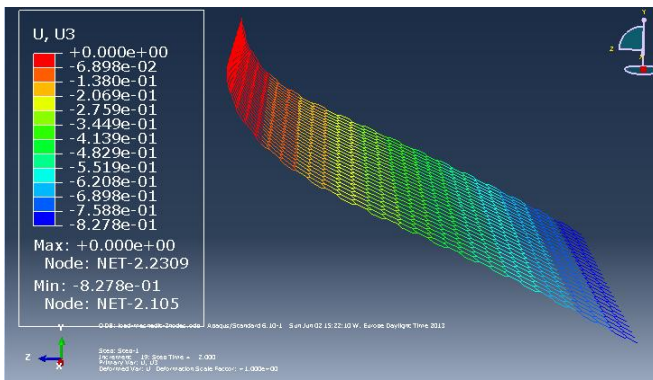


Figure 41 Deformation of model in ABAQUS (F = 11.896 N, V = 0.38 m/s)

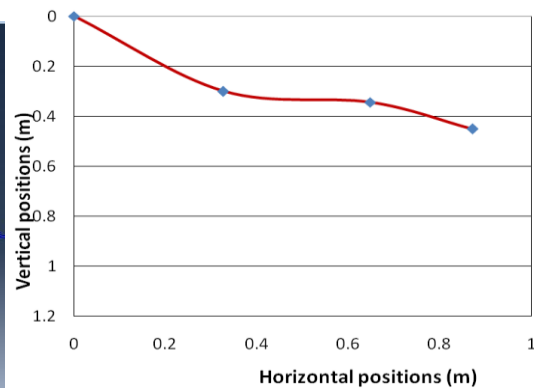
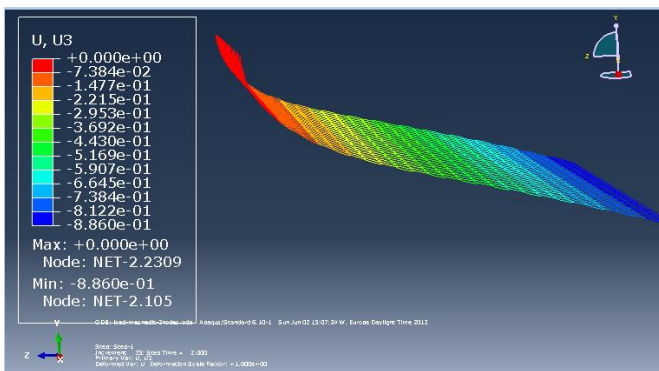


Figure 42 Deformation of model in ABAQUS (F = 17.922 N, V = 0.5 m/s)

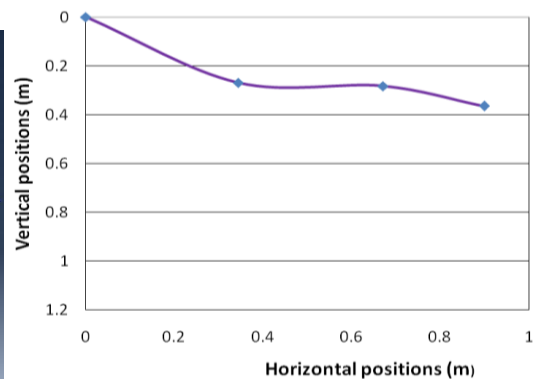
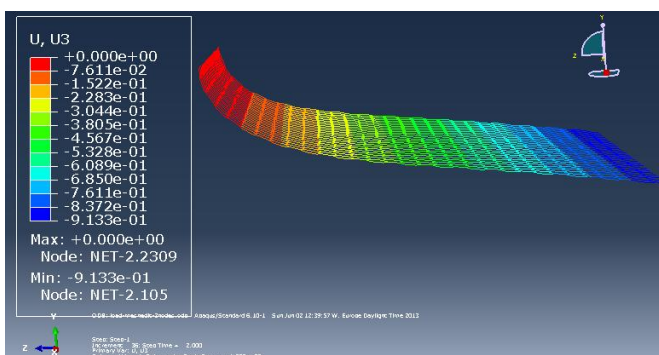


Figure 43 Deformation of model in ABAQUS (F = 25.636 N, V = 0.63 m/s)

Rotation

Table 15 outlines the data for the rotational degree of freedom in x (UR1), y (UR2) and z (UR3) directions. Note that it is the UR1 that allows the bending of the net panel and hence

the largest values in the table. UR2 is associated with the local bending or deformation of the net as this corresponds to the rotation between each mesh. Since there were not force applied in the direction of UR3, the rotations in UR3 is very small and only reflects the residual stress in the nodes.

Table 15 Average rotation displacement at nodes for the different positions and under different loads

| Position | Rotational displacement [rad] | Forces [N] | | | | |
|----------|-------------------------------|------------|--------|--------|--------|--------|
| | | 2.631 | 6.922 | 11.896 | 17.992 | 25.636 |
| 2 | UR1 | 0.279 | 0.695 | 1.161 | 1.329 | 1.424 |
| | UR2 | -0.113 | -0.057 | -0.029 | -0.023 | -0.018 |
| | UR3 | -0.017 | -0.023 | -0.021 | -0.020 | -0.017 |
| 3 | UR1 | 0.274 | 0.641 | 1.126 | 1.319 | 1.433 |
| | UR2 | -0.125 | -0.069 | -0.029 | -0.023 | -0.017 |
| | UR3 | -0.018 | -0.024 | -0.020 | -0.020 | -0.017 |
| 4 | UR1 | 0.270 | 0.622 | 1.096 | 1.295 | 1.416 |
| | UR2 | -0.130 | -0.075 | -0.030 | -0.024 | -0.017 |
| | UR3 | -0.020 | -0.025 | -0.020 | -0.019 | -0.017 |

CHAPTER 8

DISCUSSION, CONCLUSION

8.1 Discussion

The model built in ABAQUS reaches equilibrium in terms of input loads and reaction loads, suggesting that the model is consistent with the principles of finite element methods. Furthermore, the analysis is according to the Hooke's law which states that the material is elastic.

The construction of the PET net panel used in this study has extra stiffness in the vertical direction given by the two twisted vertical bars. It also allows the mesh to rotate around the x-y plane, giving more flexibility to redistribute the stress. In the modeling, this extra stiffness was given by constraining degrees of freedom at the nodes. Based on the three different type of node freedoms used in this study (refer to the 3 cases in section 6.2), case 3 gives the best results when compare to the experiments. In case 1 and case 2, the nodes (3 nodes in case 1 and 2 nodes in case 2) were modeled with free rotation, and therefore imposed more flexibility than the actual net. On the contrary, by just allowing the middle node to rotate, while the other two follows the movement in the vertical bar, case 3 gave a better representation of the actual net.

Comparing the deformation results with SINTEF experiment (Figure 38), there are slight differences in the response of the structure. These differences may rise due to the simplification of the vertical bar in the modeling, initial position in the experiment, or due to hydrodynamic effects. In the experiment of Gansel et al., 2013 they also found differences between the experiment and the model using FhSim, and it is concluded that the deformation of the net panels with bending stiffness are affected by many factors, such as elasticity of the net material, its construction, density and initial deformations of net panel (initial position).

The PET net panel modeled in ABAQUS was subjected to static forces corresponding to the drag forces from the experiment (normal to the panel). In the analysis, it was used this total force and evenly distributed to the entire structure perpendicular to the element. However, if we consider hydrodynamic forces, it is known that the hydrodynamic force is a function of the solidity and the angle of attack of the velocity, which will be different at different vertical positions due to the deflection. Therefore, it is expected that the loads applied in the upper part of the net panel be different from the loads applied on the bottom part of the net panel, which was not applied in the ABAQUS analysis. This itself could explain some of the discrepancies in the deflection, when comparing the experiment and the cases.

As seen from Figure 38, the difference in the deflection between model and experimental cases were less for larger deflections. We would like to hypothesize that this is because the deflection for stiff net, like the PET has smaller influence from the hydrodynamic parameters at larger deflections compared to the structural properties. If the deflection of the net panel in response to hydrodynamic forces can be accurately predicted by only using the structural parameters (bending stiffness), then it must be because the structural parameters alone can capture the behavior of the deformation at large deflections.

Even if the vertical bar of the PET net panel is allowed to rotate in y-direction, the biggest rotations are happening in x-direction when the panel is subjected to different loads. Thus it can be assumed that the rotation in the y-direction gives rotation between meshes while the rotation in x-direction may give the rotation of the net panel to lift. This is also confirmed by the fact that there were no translations in y-direction when the nodes were constrained from rotation. Therefore, even if the load was only applied in the z-direction (normal to the panel), we also observe the translation in the y-direction, portraying the lift force on the net panel.

Secondary discussions

Even though the objective of this thesis is to model the PET net panel in ABAQUS to see if simplified structural modeling of the net panel can predict deformation of net panels subjected to hydrodynamic forces, it was also extended the analysis to see the deformation of the net panel subjected to point loads. This scenario can be envisaged during the operation of the cage e.g. by hitting with a work boat, shark or predator attack, or even floating debris hitting the cage. To model this scenarios, it was clamped all the sides of the net panel and applied a point load in the middle of the net panel. Figure 44, shows deflection of the net panel to various point loads. As it can be seen in the Figure 44, the deflection is much localized to the area of the impact and the forces are uniformly expanded to all directions of the net panel. This is because PET net panel construction is very stiff while the twists in between the meshes give high flexibility.

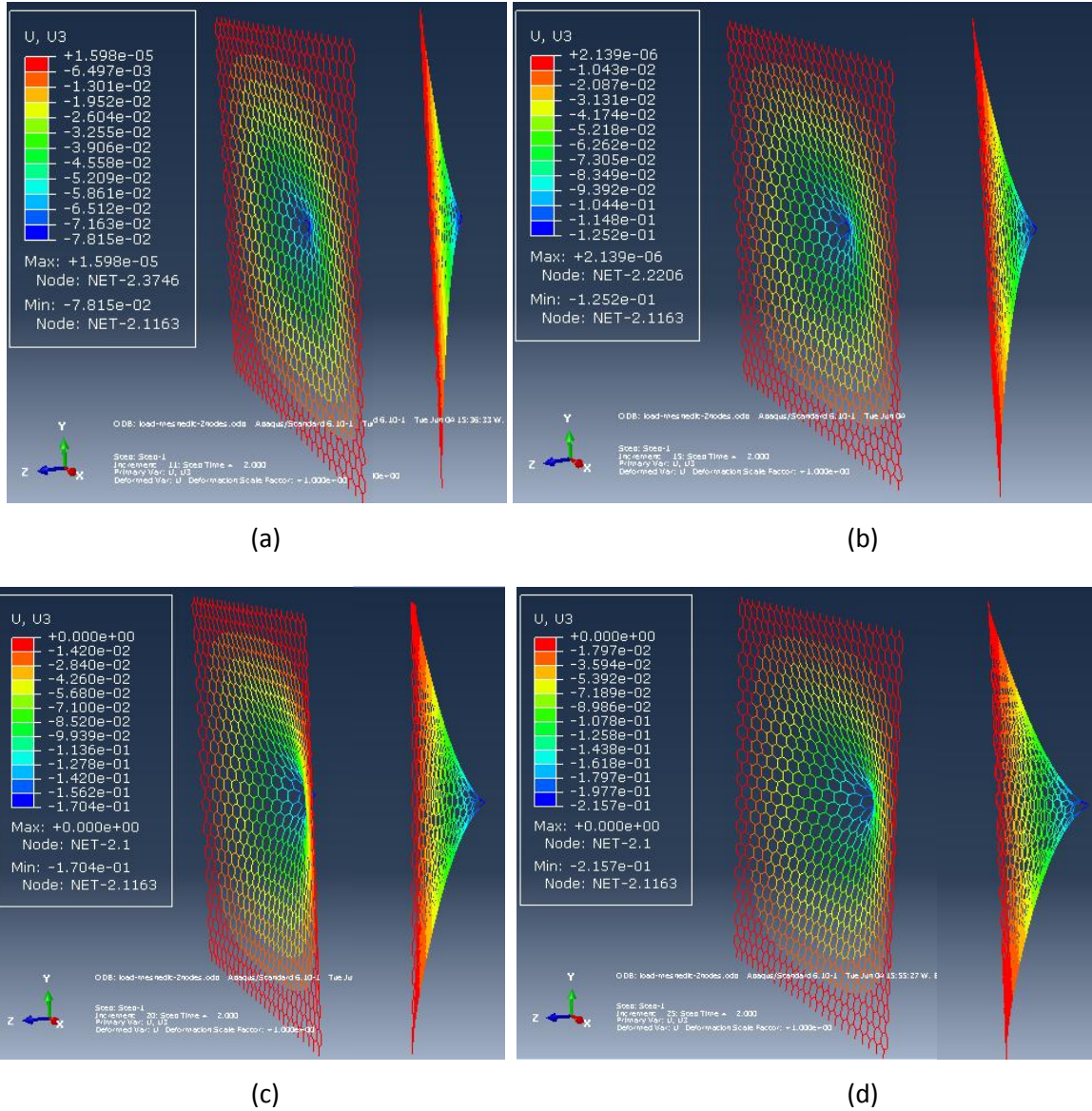


Figure 44 Deflection under different punctual loads: (a) 500N, (b) 2000N, (c) 5000N, (d) 10000N

In addition, it was also investigated if theoretical calculations based on net geometry can estimate C_D of the net panel, by comparing the C_D from the experiment. Since the basic components of net structure are twines, Lader and Enerhaug (2005) assumed that the net can be constructed as an array of cylinders. Besides, by taking into account that the drag forces on cylinders are dependent on R_n , therefore the drag forces on net structures are also dependent on R_n (Fredheim and Faltinsen, 2003). The value of R_n will then determine the drag coefficient of a cylinder (Faltinsen, 1990). The drag coefficient (C_D) of the individual cylinder in the PET net panel can be calculated by using the following Morison's formula:

$$F_N = \frac{1}{2} \rho C_D D U^2 \quad (8.1)$$

Where F is the force per unit length, D is the average diameter of the cylinder (vertical and diagonal bar = 0.00375 m), U defines velocity from the experiment and ρ is density of water. Thus Table 16 presents the result of C_D from the experiment.

Table 16 Drag coefficient of the individual cylinder from the experiment

| Flow speed [m/s] | Drag force [N/m] | C_D |
|------------------|------------------|-------|
| 0.13 | 0.055 | 1.723 |
| 0.25 | 0.144 | 1.226 |
| 0.38 | 0.247 | 0.912 |
| 0.5 | 0.373 | 0.797 |
| 0.63 | 0.532 | 0.715 |

Now if R_n is calculated by using Eq. 8.2 for the individual element of the mesh used in ABAQUS, and observe the C_D from Figure 45 which shows the relation between R_n and C_D , it can be obtained the theoretical C_D from the model (Table 17).

$$R_n = \frac{UD}{\nu} \tag{8.2}$$

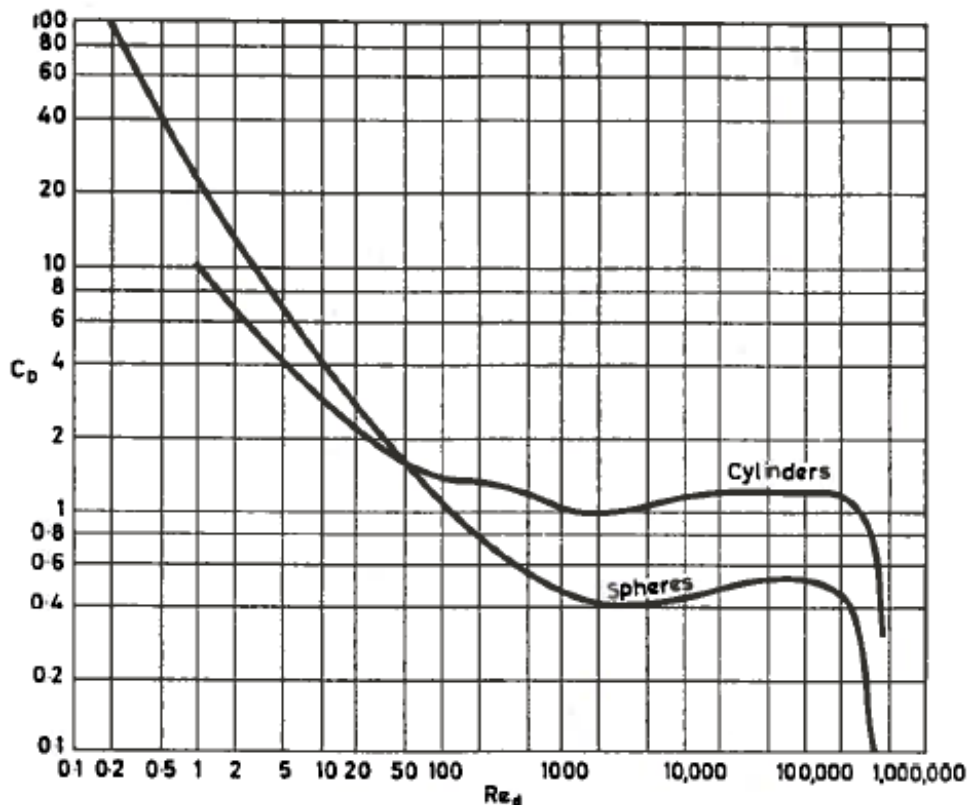


Figure 45 Drag coefficient vs Reynolds number for long circular cylinders and spheres in cross flow (Sacks et al., 1963)

Table 17 Drag coefficient based theoretical calculation

| Flow speed [m/s] | R_n [m ² /s] | CD |
|---------------------|------------------------------|------|
| 0.13 | 487.50 | 1.30 |
| 0.25 | 937.50 | 1.00 |
| 0.38 | 1425.00 | 1.00 |
| 0.5 | 1875.00 | 1.00 |
| 0.63 | 2362.50 | 1.00 |

From Table 16 and Table 17 it can be compared the theoretical and the experimental C_D . Thus the values obtained suggest that the value of C_D for PET is around 1. This value can be used for further calculation of a net cage with the same material features.

8.2 Conclusion

A PET net panel model has been built using ABAQUS according to the material properties of PET. The net panel structure is constructed by using Timoshenko beam elements, B31, and the loads were applied as a line load completely distributed over the net panel in order to simulate the uniform current. This gives a good approach for modeling this kind of structures when suggested to a load normal to the panel. Thus it can be concluded that the static analysis performed in ABAQUS is able to model the PET net panel structure used in the SINTEF experiment.

As it was expected larger displacement of the PET net panel occurs with increasing loads, which is similar to the experiments and corresponds to increased current velocity. The deformations of the net panel are affected by the node boundary conditions applied in the model. Thus the boundary condition in the vertical bar gives translation and rotational deformation, while the clamped boundary condition restricted the movement in the upper part of the net panel, and at the same time allows more deflection at the lower part. Therefore, the model is sensitive to how the net elements are modeled in ABAQUS.

It has been shown that for stiff nets such as PET, structural model in ABAQUS based on bending stiffness can predict the deformation of the net panel subjected to hydrodynamic forces, within reasonable accuracy. Hence it is possible to use the finite element software, ABAQUS, to simulate aquaculture PET nets with the purpose of estimating the net-cage deflection.

RECOMMENDATION FOR FUTURE WORK

Due to this thesis has been perform by using ABAQUS/Standard, one of the main challenges presented are the application of forces in order to simulate the experiment. In future works it is recommended to use analysis that includes the hydrodynamic effects to apply the current from the experiment.

Another improvement of the model it could be to actually include the twist part of the vertical bar, for that in future works it may be necessary to use another kind of finite elements rather than beam or trust elements.

Considering the need of information about structural behavior for aquaculture cages, the authors believe that is necessary to continue this kind of analysis and include the forces not just normal to the net panel but also applying the loads with different angles of attack as well as apply oscillation for simulate the effect of the waves.

REFERENCES

- Aarsnes, J.V., Rudi, H., Loland, G., 1990. *Current Forces on Cage, Net Deflection*. In: *Engineering for Offshore Fish Farming*, Thomas Telford, London, pp. 137–152.
- AKVAGroup, 2011-2012. *Catalogue of Cage Farming Aquaculture*. Viewed 15 May 2013. <<http://www.akvagroup.com/downloads/akva%20cage%20eng.pdf>>.
- Ashby, M.F., Jones, D.R.H., 2012. *An Introduction to Properties, Applications and Design*. *Engineering Materials-Fourth Edition*. Elsevier Ltd.
- Budynas, R.G., Nisbett, J.K., 2010. *Shigley's Mechanical Engineering Design*. Ninth Edition. McGraw-Hill companies, Inc., New York.
- Designerdata,. *Polyethylene Terephthalate (PET) Datasheet*. Viewed 10 April 2013. <<http://www.designerdata.nl/index.php?material=49&subject=2&pag=8&subpag=1&lang=en>>.
- Dessault Syst emes, 2011. *ABAQUS 6.11 Documentation*.
- Faltinsen, O. M., 1990. *Sea Loads on Ships and Offshore Structures*. Cambridge University Press.
- Fredheim, A., Faltinsen., O. M., 2003. *Hydroelastic Analysis of a Fishing Net in Steady Inflow Conditions*. 3rd International Conference on Hydroelasticity in Marine Technology, Oxford, Great Britain, University of Oxford.
- Gansel, L., Østen, J., Lien, E., Endresen, P.C., 2012. *Forces on Nets with Bending Stiffness-an Experimental Study on the Effects of Flow Speed and Angle Of Attack*. 31st International Conference on Ocean, Offshore, and Arctic Engineering (OMAE2012), July 1-6, 2012, Rio de Janeiro, Brazil.
- Gansel, L., Østen, J., E., Endresen, P.C., Føre, M., 2013. *Deformation of Nets with Bending Stiffness Normal to Uniform Currents*. 32nd International Confer-ence on Ocean, Offshore, and Arctic Engineering (OMAE2013), June 9-14, 2013, Nantes, France.
- Hughes, T.J.R., Taylor, R.L., Kanoknukulchoii, W., 1977. *A Simple and Efficient Plate Element for Bending*. *International Journal for Numerical Method in Engineering* 11, 1529-1943.

- Jensen, Ø., Gansel, L., Føre, M., Endresen, P. C., Reite, K. J., Jensen, J., and Lader, P., 2013. *Oscillation of a Net Panel with Bending Stiffness*. 32nd International Conference on Ocean, Offshore, and Arctic Engineering (OMAEO2013), June 9-14, 2013, Nantes, France.
- Kritiansen, T., Faltinsen, O. M., 2012. *Modeling of Current Loads on Aquaculture Net Cage*. Journal of Fluids and Structures 34, 218-235.
- Lader, P., Enerhaug, B., 2005. *Experimental Investigation of Forces and Geometry of a Net Cage in Uniform Flow*. IEEE Journal of Ocean Engineering 30, 79-84.
- Liu, G.R., Quek, S.S., 2003. *The Finite Element Method: A practical course*. Elsevier Science Ltd.
- Logan, D.L., 2012. *A First Course in the Finite Element Method*. Fifth Edition. Cengage Learning, Stamford, CT.
- MacNeal, R. H., 1976. *A Simple Quadrilateral Shell Element*. Computers & Structures 8, 175-183. Markopoulos, A.P., 2013. *Finite Element Method in Machining Processes*. Springer, London, New York.
- Moe, H., Fredheim, A., Hopperstad, O.S., 2010. *Structural Analysis of Aquaculture Net Cages in Current*. Journal of Fluids and Structures 26, 503-516.
- Onate, E., 2009. *Structural Analysis with Finite Element Method, Linear Static*. Volume 1: Basis and Solids. Artes Graficas Torres S.L.
- Rajput, R.K., 2005. *Basic Mechanical Engineering*. Laxmi Publication, Daryanganj, New Delhi.
- Sacks, A.H. and Burnell, J.A., 1963. *On the Use of Impact Theory of Slender Configurations Exhibiting Flow Separation*. Vidya Rept. No. 91. Vidya Research and Development, Palo Alto, Calif.
- Standard Norge, 2009. *Norwegian Standard NS 941.E: 2009 Marine Fish Farms - Requirements for Site Survey, Risk Analyses, Design, Dimensioning, Production, Installation and Operation*. Standard Norge, Lysaker.
- Steffen, J.R., 2012. *Analysis of Machines Elements Using SolidWorks Simulation*. Schroff Development Corporation.
- Sævik, S., Moan, T., Larsen, C.M., 2010. *Advanced Structural Analysis*. In: Lecture Notes TMR4305. Norwegian University of Science and Technology, Trondheim.

Tessler, A., Dong, S. B., 1981. On a Hierarchy of Conforming Timoshenko Beam Elements. *Computers & Structures* 14, 335-344.

Tsukrov, I., Drach, A., DeCew, J., Swift, M. R. and Celikkol, B., 2011. *Characterization of Geometry and Normal Drag Coefficients of Copper Nets*. *Ocean Engineering*, 38, pp. 1979-1988.

Ye, J., 2008. *Structural and Stress Analysis: Theories, Tutorials, and Examples*. Taylor & Francis.

APPENDIX

Average displacement at position (case 3)

Load 1 = 2.63 N

| Position 1 | | Position 2 | | Position 3 | |
|------------|-----------|------------|-----------|------------|-----------|
| Node label | U3 | Node label | U3 | Node label | U3 |
| 1288 | -6.09E-02 | 499 | -1.46E-01 | 7 | -2.05E-01 |
| 1289 | -5.81E-02 | 500 | -1.43E-01 | 15 | -2.14E-01 |
| 1290 | -5.52E-02 | 501 | -1.40E-01 | 23 | -2.22E-01 |
| 1292 | -5.87E-02 | 503 | -1.44E-01 | 31 | -2.31E-01 |
| 1293 | -6.16E-02 | 504 | -1.47E-01 | 39 | -2.40E-01 |
| 1294 | -6.45E-02 | 505 | -1.50E-01 | 47 | -2.49E-01 |
| 1296 | -6.78E-02 | 507 | -1.54E-01 | 55 | -2.58E-01 |
| 1297 | -6.49E-02 | 508 | -1.51E-01 | 63 | -2.68E-01 |
| 1298 | -6.19E-02 | 509 | -1.48E-01 | 71 | -2.76E-01 |
| 1300 | -6.53E-02 | 511 | -1.52E-01 | 79 | -2.85E-01 |
| 1301 | -6.83E-02 | 512 | -1.55E-01 | 87 | -2.94E-01 |
| 1302 | -7.13E-02 | 513 | -1.58E-01 | 95 | -3.02E-01 |
| 1304 | -7.49E-02 | 515 | -1.62E-01 | 103 | -3.06E-01 |
| 1305 | -7.19E-02 | 516 | -1.59E-01 | 104 | -3.09E-01 |
| 1306 | -6.89E-02 | 517 | -1.56E-01 | 105 | -3.13E-01 |
| 1308 | -7.26E-02 | 519 | -1.60E-01 | 109 | -2.01E-01 |
| 1309 | -7.56E-02 | 520 | -1.63E-01 | 110 | -2.08E-01 |
| 1310 | -7.86E-02 | 521 | -1.66E-01 | 111 | -2.11E-01 |
| 1312 | -8.24E-02 | 523 | -1.70E-01 | 112 | -2.09E-01 |
| 1313 | -7.94E-02 | 524 | -1.67E-01 | 115 | -2.17E-01 |
| 1314 | -7.64E-02 | 525 | -1.64E-01 | 116 | -2.20E-01 |
| 1316 | -8.03E-02 | 527 | -1.68E-01 | 117 | -2.18E-01 |
| 1317 | -8.33E-02 | 528 | -1.71E-01 | 120 | -2.25E-01 |
| 1318 | -8.63E-02 | 529 | -1.74E-01 | 121 | -2.28E-01 |
| 1320 | -9.03E-02 | 531 | -1.78E-01 | 122 | -2.27E-01 |
| 1321 | -8.72E-02 | 532 | -1.75E-01 | 125 | -2.34E-01 |
| 1322 | -8.42E-02 | 533 | -1.72E-01 | 126 | -2.37E-01 |
| 1324 | -8.83E-02 | 535 | -1.76E-01 | 127 | -2.36E-01 |
| 1325 | -9.13E-02 | 536 | -1.79E-01 | 130 | -2.43E-01 |
| 1326 | -9.43E-02 | 537 | -1.83E-01 | 131 | -2.46E-01 |
| 1328 | -9.84E-02 | 539 | -1.87E-01 | 132 | -2.45E-01 |
| 1329 | -9.53E-02 | 540 | -1.84E-01 | 135 | -2.52E-01 |
| 1330 | -9.23E-02 | 541 | -1.81E-01 | 136 | -2.56E-01 |
| 1332 | -9.64E-02 | 543 | -1.85E-01 | 137 | -2.54E-01 |
| 1333 | -9.94E-02 | 544 | -1.88E-01 | 140 | -2.62E-01 |
| 1334 | -1.02E-01 | 545 | -1.91E-01 | 141 | -2.65E-01 |
| 1336 | -1.07E-01 | 547 | -1.95E-01 | 142 | -2.63E-01 |

| | | | | | |
|------|-----------|-----|-----------|-----|-----------|
| 1337 | -1.04E-01 | 548 | -1.92E-01 | 145 | -2.71E-01 |
| 1338 | -1.00E-01 | 549 | -1.89E-01 | 146 | -2.74E-01 |
| 1340 | -1.05E-01 | 551 | -1.93E-01 | 147 | -2.72E-01 |
| 1341 | -1.08E-01 | 552 | -1.97E-01 | 150 | -2.80E-01 |
| 1342 | -1.11E-01 | 553 | -2.00E-01 | 151 | -2.83E-01 |
| 1344 | -1.15E-01 | 555 | -2.04E-01 | 152 | -2.81E-01 |
| 1345 | -1.12E-01 | 556 | -2.01E-01 | 155 | -2.88E-01 |
| 1346 | -1.09E-01 | 557 | -1.98E-01 | 156 | -2.92E-01 |
| 1348 | -1.13E-01 | 559 | -2.02E-01 | 157 | -2.90E-01 |
| 1349 | -1.16E-01 | 560 | -2.05E-01 | 160 | -2.97E-01 |
| 1350 | -1.19E-01 | 561 | -2.09E-01 | 161 | -3.00E-01 |
| 1352 | -1.23E-01 | 563 | -2.13E-01 | 162 | -2.98E-01 |
| 1353 | -1.20E-01 | 564 | -2.10E-01 | 165 | -3.05E-01 |
| 1354 | -1.17E-01 | 565 | -2.07E-01 | 166 | -3.08E-01 |
| 1356 | -1.21E-01 | 567 | -2.11E-01 | 274 | -2.04E-01 |
| 1357 | -1.24E-01 | 568 | -2.14E-01 | 275 | -2.06E-01 |
| 1358 | -1.27E-01 | 569 | -2.17E-01 | 278 | -2.12E-01 |
| 1360 | -1.31E-01 | 571 | -2.22E-01 | 279 | -2.15E-01 |
| 1361 | -1.28E-01 | 572 | -2.19E-01 | 282 | -2.21E-01 |
| 1362 | -1.25E-01 | 573 | -2.16E-01 | 283 | -2.24E-01 |
| 1364 | -1.28E-01 | 575 | -2.20E-01 | 286 | -2.30E-01 |
| 1365 | -1.32E-01 | 576 | -2.23E-01 | 287 | -2.33E-01 |
| 1366 | -1.35E-01 | 577 | -2.26E-01 | 290 | -2.39E-01 |
| 1368 | -1.39E-01 | 579 | -2.31E-01 | 291 | -2.42E-01 |
| 1369 | -1.36E-01 | 580 | -2.27E-01 | 294 | -2.48E-01 |
| 1370 | -1.32E-01 | 581 | -2.24E-01 | 295 | -2.51E-01 |
| 1372 | -1.36E-01 | 583 | -2.29E-01 | 298 | -2.57E-01 |
| 1373 | -1.39E-01 | 584 | -2.32E-01 | 299 | -2.60E-01 |
| 1374 | -1.43E-01 | 585 | -2.35E-01 | 302 | -2.66E-01 |
| 1376 | -1.47E-01 | 587 | -2.39E-01 | 303 | -2.69E-01 |
| 1377 | -1.43E-01 | 588 | -2.36E-01 | 306 | -2.75E-01 |
| 1378 | -1.40E-01 | 589 | -2.33E-01 | 307 | -2.78E-01 |
| 1380 | -1.43E-01 | 591 | -2.37E-01 | 310 | -2.84E-01 |
| 1381 | -1.47E-01 | 592 | -2.40E-01 | 311 | -2.87E-01 |
| 1382 | -1.50E-01 | 593 | -2.43E-01 | 314 | -2.93E-01 |
| 1384 | -1.54E-01 | 595 | -2.47E-01 | 315 | -2.96E-01 |
| 1385 | -1.50E-01 | 596 | -2.44E-01 | 318 | -3.01E-01 |
| 1386 | -1.46E-01 | 597 | -2.41E-01 | 319 | -3.04E-01 |
| 1388 | -1.50E-01 | 599 | -2.45E-01 | | |
| 1389 | -1.54E-01 | 600 | -2.49E-01 | | |
| 1390 | -1.57E-01 | 601 | -2.52E-01 | | |

AVERAGE

-1.06E-01

-1.95E-01

-2.57E-01

Load 2 = 6.9 N

| Position 1 | | Position 2 | | Position 3 | |
|------------|-----------|------------|-----------|------------|-----------|
| Node label | U3 | Node label | U3 | Node label | U3 |
| 1288 | -2.14E-01 | 499 | -4.14E-01 | 7 | -5.37E-01 |
| 1289 | -2.07E-01 | 500 | -4.07E-01 | 15 | -5.42E-01 |
| 1290 | -2.00E-01 | 501 | -4.00E-01 | 23 | -5.46E-01 |
| 1292 | -2.02E-01 | 503 | -4.02E-01 | 31 | -5.50E-01 |
| 1293 | -2.09E-01 | 504 | -4.09E-01 | 39 | -5.55E-01 |
| 1294 | -2.16E-01 | 505 | -4.16E-01 | 47 | -5.59E-01 |
| 1296 | -2.18E-01 | 507 | -4.18E-01 | 55 | -5.64E-01 |
| 1297 | -2.11E-01 | 508 | -4.11E-01 | 63 | -5.68E-01 |
| 1298 | -2.03E-01 | 509 | -4.05E-01 | 71 | -5.73E-01 |
| 1300 | -2.05E-01 | 511 | -4.07E-01 | 79 | -5.78E-01 |
| 1301 | -2.12E-01 | 512 | -4.13E-01 | 87 | -5.82E-01 |
| 1302 | -2.20E-01 | 513 | -4.20E-01 | 95 | -5.87E-01 |
| 1304 | -2.21E-01 | 515 | -4.22E-01 | 103 | -5.89E-01 |
| 1305 | -2.14E-01 | 516 | -4.15E-01 | 104 | -5.96E-01 |
| 1306 | -2.07E-01 | 517 | -4.09E-01 | 105 | -6.03E-01 |
| 1308 | -2.08E-01 | 519 | -4.11E-01 | 109 | -5.35E-01 |
| 1309 | -2.16E-01 | 520 | -4.17E-01 | 110 | -5.44E-01 |
| 1310 | -2.23E-01 | 521 | -4.24E-01 | 111 | -5.50E-01 |
| 1312 | -2.25E-01 | 523 | -4.26E-01 | 112 | -5.39E-01 |
| 1313 | -2.18E-01 | 524 | -4.19E-01 | 115 | -5.48E-01 |
| 1314 | -2.10E-01 | 525 | -4.13E-01 | 116 | -5.55E-01 |
| 1316 | -2.12E-01 | 527 | -4.15E-01 | 117 | -5.44E-01 |
| 1317 | -2.19E-01 | 528 | -4.21E-01 | 120 | -5.53E-01 |
| 1318 | -2.27E-01 | 529 | -4.28E-01 | 121 | -5.59E-01 |
| 1320 | -2.28E-01 | 531 | -4.30E-01 | 122 | -5.48E-01 |
| 1321 | -2.21E-01 | 532 | -4.23E-01 | 125 | -5.57E-01 |
| 1322 | -2.14E-01 | 533 | -4.17E-01 | 126 | -5.64E-01 |
| 1324 | -2.16E-01 | 535 | -4.19E-01 | 127 | -5.53E-01 |
| 1325 | -2.23E-01 | 536 | -4.25E-01 | 130 | -5.61E-01 |
| 1326 | -2.30E-01 | 537 | -4.32E-01 | 131 | -5.68E-01 |
| 1328 | -2.32E-01 | 539 | -4.34E-01 | 132 | -5.57E-01 |
| 1329 | -2.25E-01 | 540 | -4.28E-01 | 135 | -5.66E-01 |
| 1330 | -2.17E-01 | 541 | -4.21E-01 | 136 | -5.73E-01 |
| 1332 | -2.19E-01 | 543 | -4.23E-01 | 137 | -5.62E-01 |
| 1333 | -2.27E-01 | 544 | -4.30E-01 | 140 | -5.71E-01 |
| 1334 | -2.34E-01 | 545 | -4.36E-01 | 141 | -5.77E-01 |
| 1336 | -2.36E-01 | 547 | -4.38E-01 | 142 | -5.66E-01 |
| 1337 | -2.28E-01 | 548 | -4.32E-01 | 145 | -5.75E-01 |
| 1338 | -2.21E-01 | 549 | -4.25E-01 | 146 | -5.82E-01 |
| 1340 | -2.23E-01 | 551 | -4.27E-01 | 147 | -5.71E-01 |
| 1341 | -2.30E-01 | 552 | -4.34E-01 | 150 | -5.80E-01 |
| 1342 | -2.37E-01 | 553 | -4.40E-01 | 151 | -5.86E-01 |
| 1344 | -2.39E-01 | 555 | -4.43E-01 | 152 | -5.75E-01 |

| | | | | | |
|------|-----------|-----|-----------|-----|-----------|
| 1345 | -2.32E-01 | 556 | -4.36E-01 | 155 | -5.84E-01 |
| 1346 | -2.25E-01 | 557 | -4.29E-01 | 156 | -5.91E-01 |
| 1348 | -2.26E-01 | 559 | -4.31E-01 | 157 | -5.80E-01 |
| 1349 | -2.34E-01 | 560 | -4.38E-01 | 160 | -5.89E-01 |
| 1350 | -2.41E-01 | 561 | -4.45E-01 | 161 | -5.96E-01 |
| 1352 | -2.43E-01 | 563 | -4.47E-01 | 162 | -5.84E-01 |
| 1353 | -2.35E-01 | 564 | -4.40E-01 | 165 | -5.93E-01 |
| 1354 | -2.28E-01 | 565 | -4.33E-01 | 166 | -6.00E-01 |
| 1356 | -2.30E-01 | 567 | -4.35E-01 | 274 | -5.41E-01 |
| 1357 | -2.37E-01 | 568 | -4.42E-01 | 275 | -5.48E-01 |
| 1358 | -2.45E-01 | 569 | -4.49E-01 | 278 | -5.46E-01 |
| 1360 | -2.46E-01 | 571 | -4.51E-01 | 279 | -5.53E-01 |
| 1361 | -2.39E-01 | 572 | -4.44E-01 | 282 | -5.50E-01 |
| 1362 | -2.32E-01 | 573 | -4.37E-01 | 283 | -5.57E-01 |
| 1364 | -2.33E-01 | 575 | -4.39E-01 | 286 | -5.55E-01 |
| 1365 | -2.41E-01 | 576 | -4.46E-01 | 287 | -5.61E-01 |
| 1366 | -2.48E-01 | 577 | -4.53E-01 | 290 | -5.59E-01 |
| 1368 | -2.50E-01 | 579 | -4.55E-01 | 291 | -5.66E-01 |
| 1369 | -2.43E-01 | 580 | -4.48E-01 | 294 | -5.64E-01 |
| 1370 | -2.35E-01 | 581 | -4.41E-01 | 295 | -5.70E-01 |
| 1372 | -2.37E-01 | 583 | -4.43E-01 | 298 | -5.68E-01 |
| 1373 | -2.44E-01 | 584 | -4.50E-01 | 299 | -5.75E-01 |
| 1374 | -2.52E-01 | 585 | -4.57E-01 | 302 | -5.73E-01 |
| 1376 | -2.54E-01 | 587 | -4.59E-01 | 303 | -5.80E-01 |
| 1377 | -2.46E-01 | 588 | -4.52E-01 | 306 | -5.77E-01 |
| 1378 | -2.39E-01 | 589 | -4.45E-01 | 307 | -5.84E-01 |
| 1380 | -2.41E-01 | 591 | -4.47E-01 | 310 | -5.82E-01 |
| 1381 | -2.48E-01 | 592 | -4.54E-01 | 311 | -5.89E-01 |
| 1382 | -2.55E-01 | 593 | -4.61E-01 | 314 | -5.87E-01 |
| 1384 | -2.57E-01 | 595 | -4.63E-01 | 315 | -5.93E-01 |
| 1385 | -2.50E-01 | 596 | -4.56E-01 | 318 | -5.91E-01 |
| 1386 | -2.42E-01 | 597 | -4.49E-01 | 319 | -5.98E-01 |
| 1388 | -2.44E-01 | 599 | -4.52E-01 | | |
| 1389 | -2.52E-01 | 600 | -4.59E-01 | | |
| 1390 | -2.59E-01 | 601 | -4.66E-01 | | |

| | | | |
|----------------|------------------|------------------|------------------|
| AVERAGE | -2.29E-01 | -4.33E-01 | -5.68E-01 |
|----------------|------------------|------------------|------------------|

Load 3 = 11.9 N

| Position 1 | | Position 2 | | Position 3 | |
|------------|-----------|------------|-----------|------------|-----------|
| Node label | U3 | Node label | U3 | Node label | U3 |
| 1288 | -3.05E-01 | 499 | -6.06E-01 | 7 | -7.93E-01 |
| 1289 | -2.94E-01 | 500 | -5.95E-01 | 15 | -7.94E-01 |

| | | | | | |
|------|-----------|-----|-----------|-----|-----------|
| 1290 | -2.84E-01 | 501 | -5.85E-01 | 23 | -7.95E-01 |
| 1292 | -2.84E-01 | 503 | -5.86E-01 | 31 | -7.96E-01 |
| 1293 | -2.95E-01 | 504 | -5.96E-01 | 39 | -7.98E-01 |
| 1294 | -3.05E-01 | 505 | -6.06E-01 | 47 | -7.99E-01 |
| 1296 | -3.06E-01 | 507 | -6.07E-01 | 55 | -8.00E-01 |
| 1297 | -2.95E-01 | 508 | -5.97E-01 | 63 | -8.01E-01 |
| 1298 | -2.85E-01 | 509 | -5.86E-01 | 71 | -8.03E-01 |
| 1300 | -2.86E-01 | 511 | -5.87E-01 | 79 | -8.04E-01 |
| 1301 | -2.96E-01 | 512 | -5.97E-01 | 87 | -8.05E-01 |
| 1302 | -3.07E-01 | 513 | -6.08E-01 | 95 | -8.07E-01 |
| 1304 | -3.07E-01 | 515 | -6.08E-01 | 103 | -8.07E-01 |
| 1305 | -2.97E-01 | 516 | -5.98E-01 | 104 | -8.18E-01 |
| 1306 | -2.86E-01 | 517 | -5.87E-01 | 105 | -8.28E-01 |
| 1308 | -2.87E-01 | 519 | -5.88E-01 | 109 | -7.92E-01 |
| 1309 | -2.97E-01 | 520 | -5.98E-01 | 110 | -8.03E-01 |
| 1310 | -3.08E-01 | 521 | -6.09E-01 | 111 | -8.13E-01 |
| 1312 | -3.08E-01 | 523 | -6.09E-01 | 112 | -7.93E-01 |
| 1313 | -2.98E-01 | 524 | -5.99E-01 | 115 | -8.04E-01 |
| 1314 | -2.87E-01 | 525 | -5.89E-01 | 116 | -8.14E-01 |
| 1316 | -2.88E-01 | 527 | -5.89E-01 | 117 | -7.94E-01 |
| 1317 | -2.99E-01 | 528 | -6.00E-01 | 120 | -8.05E-01 |
| 1318 | -3.09E-01 | 529 | -6.10E-01 | 121 | -8.16E-01 |
| 1320 | -3.10E-01 | 531 | -6.11E-01 | 122 | -7.96E-01 |
| 1321 | -2.99E-01 | 532 | -6.00E-01 | 125 | -8.07E-01 |
| 1322 | -2.89E-01 | 533 | -5.90E-01 | 126 | -8.17E-01 |
| 1324 | -2.89E-01 | 535 | -5.91E-01 | 127 | -7.97E-01 |
| 1325 | -3.00E-01 | 536 | -6.01E-01 | 130 | -8.08E-01 |
| 1326 | -3.10E-01 | 537 | -6.11E-01 | 131 | -8.18E-01 |
| 1328 | -3.11E-01 | 539 | -6.12E-01 | 132 | -7.98E-01 |
| 1329 | -3.00E-01 | 540 | -6.02E-01 | 135 | -8.09E-01 |
| 1330 | -2.90E-01 | 541 | -5.91E-01 | 136 | -8.19E-01 |
| 1332 | -2.91E-01 | 543 | -5.92E-01 | 137 | -8.00E-01 |
| 1333 | -3.01E-01 | 544 | -6.02E-01 | 140 | -8.10E-01 |
| 1334 | -3.12E-01 | 545 | -6.13E-01 | 141 | -8.21E-01 |
| 1336 | -3.12E-01 | 547 | -6.13E-01 | 142 | -8.01E-01 |
| 1337 | -3.02E-01 | 548 | -6.03E-01 | 145 | -8.12E-01 |
| 1338 | -2.91E-01 | 549 | -5.93E-01 | 146 | -8.22E-01 |
| 1340 | -2.92E-01 | 551 | -5.93E-01 | 147 | -8.02E-01 |
| 1341 | -3.02E-01 | 552 | -6.04E-01 | 150 | -8.13E-01 |
| 1342 | -3.13E-01 | 553 | -6.14E-01 | 151 | -8.23E-01 |
| 1344 | -3.14E-01 | 555 | -6.15E-01 | 152 | -8.03E-01 |
| 1345 | -3.03E-01 | 556 | -6.04E-01 | 155 | -8.14E-01 |
| 1346 | -2.92E-01 | 557 | -5.94E-01 | 156 | -8.25E-01 |
| 1348 | -2.93E-01 | 559 | -5.94E-01 | 157 | -8.05E-01 |
| 1349 | -3.04E-01 | 560 | -6.05E-01 | 160 | -8.16E-01 |
| 1350 | -3.14E-01 | 561 | -6.15E-01 | 161 | -8.26E-01 |

| | | | | | |
|----------------|-----------|------------------|------------------|------------------|-----------|
| 1352 | -3.15E-01 | 563 | -6.16E-01 | 162 | -8.06E-01 |
| 1353 | -3.04E-01 | 564 | -6.05E-01 | 165 | -8.17E-01 |
| 1354 | -2.94E-01 | 565 | -5.95E-01 | 166 | -8.27E-01 |
| 1356 | -2.94E-01 | 567 | -5.96E-01 | 274 | -8.02E-01 |
| 1357 | -3.05E-01 | 568 | -6.06E-01 | 275 | -8.12E-01 |
| 1358 | -3.15E-01 | 569 | -6.16E-01 | 278 | -8.03E-01 |
| 1360 | -3.16E-01 | 571 | -6.17E-01 | 279 | -8.14E-01 |
| 1361 | -3.05E-01 | 572 | -6.07E-01 | 282 | -8.05E-01 |
| 1362 | -2.95E-01 | 573 | -5.96E-01 | 283 | -8.15E-01 |
| 1364 | -2.96E-01 | 575 | -5.97E-01 | 286 | -8.06E-01 |
| 1365 | -3.06E-01 | 576 | -6.07E-01 | 287 | -8.16E-01 |
| 1366 | -3.17E-01 | 577 | -6.18E-01 | 290 | -8.07E-01 |
| 1368 | -3.17E-01 | 579 | -6.18E-01 | 291 | -8.17E-01 |
| 1369 | -3.07E-01 | 580 | -6.08E-01 | 294 | -8.09E-01 |
| 1370 | -2.96E-01 | 581 | -5.98E-01 | 295 | -8.19E-01 |
| 1372 | -2.97E-01 | 583 | -5.98E-01 | 298 | -8.10E-01 |
| 1373 | -3.07E-01 | 584 | -6.09E-01 | 299 | -8.20E-01 |
| 1374 | -3.18E-01 | 585 | -6.19E-01 | 302 | -8.11E-01 |
| 1376 | -3.19E-01 | 587 | -6.20E-01 | 303 | -8.21E-01 |
| 1377 | -3.08E-01 | 588 | -6.09E-01 | 306 | -8.12E-01 |
| 1378 | -2.97E-01 | 589 | -5.99E-01 | 307 | -8.23E-01 |
| 1380 | -2.98E-01 | 591 | -6.00E-01 | 310 | -8.14E-01 |
| 1381 | -3.09E-01 | 592 | -6.10E-01 | 311 | -8.24E-01 |
| 1382 | -3.19E-01 | 593 | -6.20E-01 | 314 | -8.15E-01 |
| 1384 | -3.20E-01 | 595 | -6.21E-01 | 315 | -8.25E-01 |
| 1385 | -3.09E-01 | 596 | -6.11E-01 | 318 | -8.16E-01 |
| 1386 | -2.99E-01 | 597 | -6.00E-01 | 319 | -8.26E-01 |
| 1388 | -3.00E-01 | 599 | -6.01E-01 | | |
| 1389 | -3.10E-01 | 600 | -6.11E-01 | | |
| 1390 | -3.21E-01 | 601 | -6.22E-01 | | |
| AVERAGE | | -3.02E-01 | -6.03E-01 | -8.10E-01 | |

Load 4 = 17.99 N

| Position 1 | | Position 2 | | Position 3 | |
|------------|-----------|------------|-----------|------------|-----------|
| Node label | U3 | Node label | U3 | Node label | U3 |
| 1288 | -3.33E-01 | 499 | -6.54E-01 | 7 | -8.55E-01 |
| 1289 | -3.22E-01 | 500 | -6.43E-01 | 15 | -8.56E-01 |
| 1290 | -3.11E-01 | 501 | -6.32E-01 | 23 | -8.57E-01 |
| 1292 | -3.11E-01 | 503 | -6.32E-01 | 31 | -8.57E-01 |
| 1293 | -3.23E-01 | 504 | -6.43E-01 | 39 | -8.58E-01 |
| 1294 | -3.34E-01 | 505 | -6.54E-01 | 47 | -8.59E-01 |
| 1296 | -3.34E-01 | 507 | -6.55E-01 | 55 | -8.60E-01 |
| 1297 | -3.23E-01 | 508 | -6.44E-01 | 63 | -8.61E-01 |

| | | | | | |
|------|-----------|-----|-----------|-----|-----------|
| 1298 | -3.12E-01 | 509 | -6.32E-01 | 71 | -8.61E-01 |
| 1300 | -3.12E-01 | 511 | -6.33E-01 | 79 | -8.62E-01 |
| 1301 | -3.23E-01 | 512 | -6.44E-01 | 87 | -8.63E-01 |
| 1302 | -3.34E-01 | 513 | -6.55E-01 | 95 | -8.64E-01 |
| 1304 | -3.35E-01 | 515 | -6.55E-01 | 103 | -8.64E-01 |
| 1305 | -3.24E-01 | 516 | -6.44E-01 | 104 | -8.75E-01 |
| 1306 | -3.13E-01 | 517 | -6.33E-01 | 105 | -8.86E-01 |
| 1308 | -3.13E-01 | 519 | -6.34E-01 | 109 | -8.55E-01 |
| 1309 | -3.24E-01 | 520 | -6.45E-01 | 110 | -8.66E-01 |
| 1310 | -3.35E-01 | 521 | -6.56E-01 | 111 | -8.77E-01 |
| 1312 | -3.36E-01 | 523 | -6.56E-01 | 112 | -8.56E-01 |
| 1313 | -3.24E-01 | 524 | -6.45E-01 | 115 | -8.67E-01 |
| 1314 | -3.13E-01 | 525 | -6.34E-01 | 116 | -8.78E-01 |
| 1316 | -3.14E-01 | 527 | -6.34E-01 | 117 | -8.56E-01 |
| 1317 | -3.25E-01 | 528 | -6.46E-01 | 120 | -8.68E-01 |
| 1318 | -3.36E-01 | 529 | -6.57E-01 | 121 | -8.79E-01 |
| 1320 | -3.36E-01 | 531 | -6.57E-01 | 122 | -8.57E-01 |
| 1321 | -3.25E-01 | 532 | -6.46E-01 | 125 | -8.69E-01 |
| 1322 | -3.14E-01 | 533 | -6.35E-01 | 126 | -8.80E-01 |
| 1324 | -3.14E-01 | 535 | -6.35E-01 | 127 | -8.58E-01 |
| 1325 | -3.26E-01 | 536 | -6.46E-01 | 130 | -8.69E-01 |
| 1326 | -3.37E-01 | 537 | -6.57E-01 | 131 | -8.80E-01 |
| 1328 | -3.37E-01 | 539 | -6.58E-01 | 132 | -8.59E-01 |
| 1329 | -3.26E-01 | 540 | -6.47E-01 | 135 | -8.70E-01 |
| 1330 | -3.15E-01 | 541 | -6.36E-01 | 136 | -8.81E-01 |
| 1332 | -3.15E-01 | 543 | -6.36E-01 | 137 | -8.59E-01 |
| 1333 | -3.26E-01 | 544 | -6.47E-01 | 140 | -8.71E-01 |
| 1334 | -3.38E-01 | 545 | -6.58E-01 | 141 | -8.82E-01 |
| 1336 | -3.38E-01 | 547 | -6.59E-01 | 142 | -8.60E-01 |
| 1337 | -3.27E-01 | 548 | -6.47E-01 | 145 | -8.72E-01 |
| 1338 | -3.16E-01 | 549 | -6.36E-01 | 146 | -8.83E-01 |
| 1340 | -3.16E-01 | 551 | -6.37E-01 | 147 | -8.61E-01 |
| 1341 | -3.27E-01 | 552 | -6.48E-01 | 150 | -8.72E-01 |
| 1342 | -3.38E-01 | 553 | -6.59E-01 | 151 | -8.83E-01 |
| 1344 | -3.39E-01 | 555 | -6.59E-01 | 152 | -8.62E-01 |
| 1345 | -3.27E-01 | 556 | -6.48E-01 | 155 | -8.73E-01 |
| 1346 | -3.16E-01 | 557 | -6.37E-01 | 156 | -8.84E-01 |
| 1348 | -3.17E-01 | 559 | -6.38E-01 | 157 | -8.62E-01 |
| 1349 | -3.28E-01 | 560 | -6.49E-01 | 160 | -8.74E-01 |
| 1350 | -3.39E-01 | 561 | -6.60E-01 | 161 | -8.85E-01 |
| 1352 | -3.39E-01 | 563 | -6.60E-01 | 162 | -8.63E-01 |
| 1353 | -3.28E-01 | 564 | -6.49E-01 | 165 | -8.75E-01 |
| 1354 | -3.17E-01 | 565 | -6.38E-01 | 166 | -8.86E-01 |
| 1356 | -3.17E-01 | 567 | -6.38E-01 | 274 | -8.66E-01 |
| 1357 | -3.29E-01 | 568 | -6.49E-01 | 275 | -8.77E-01 |
| 1358 | -3.40E-01 | 569 | -6.61E-01 | 278 | -8.67E-01 |

| | | | | | |
|------|-----------|-----|-----------|-----|-----------|
| 1360 | -3.40E-01 | 571 | -6.61E-01 | 279 | -8.78E-01 |
| 1361 | -3.29E-01 | 572 | -6.50E-01 | 282 | -8.67E-01 |
| 1362 | -3.18E-01 | 573 | -6.39E-01 | 283 | -8.78E-01 |
| 1364 | -3.18E-01 | 575 | -6.39E-01 | 286 | -8.68E-01 |
| 1365 | -3.29E-01 | 576 | -6.50E-01 | 287 | -8.79E-01 |
| 1366 | -3.41E-01 | 577 | -6.61E-01 | 290 | -8.69E-01 |
| 1368 | -3.41E-01 | 579 | -6.62E-01 | 291 | -8.80E-01 |
| 1369 | -3.30E-01 | 580 | -6.51E-01 | 294 | -8.70E-01 |
| 1370 | -3.19E-01 | 581 | -6.39E-01 | 295 | -8.81E-01 |
| 1372 | -3.19E-01 | 583 | -6.40E-01 | 298 | -8.70E-01 |
| 1373 | -3.30E-01 | 584 | -6.51E-01 | 299 | -8.82E-01 |
| 1374 | -3.41E-01 | 585 | -6.62E-01 | 302 | -8.71E-01 |
| 1376 | -3.42E-01 | 587 | -6.62E-01 | 303 | -8.82E-01 |
| 1377 | -3.31E-01 | 588 | -6.51E-01 | 306 | -8.72E-01 |
| 1378 | -3.19E-01 | 589 | -6.40E-01 | 307 | -8.83E-01 |
| 1380 | -3.20E-01 | 591 | -6.41E-01 | 310 | -8.73E-01 |
| 1381 | -3.31E-01 | 592 | -6.52E-01 | 311 | -8.84E-01 |
| 1382 | -3.42E-01 | 593 | -6.63E-01 | 314 | -8.74E-01 |
| 1384 | -3.43E-01 | 595 | -6.63E-01 | 315 | -8.85E-01 |
| 1385 | -3.31E-01 | 596 | -6.52E-01 | 318 | -8.74E-01 |
| 1386 | -3.20E-01 | 597 | -6.41E-01 | 319 | -8.85E-01 |
| 1388 | -3.20E-01 | 599 | -6.41E-01 | | |
| 1389 | -3.32E-01 | 600 | -6.52E-01 | | |
| 1390 | -3.43E-01 | 601 | -6.63E-01 | | |

AVERAGE

-3.27E-01

-6.48E-01

-8.70E-01

Load 2 = 25.6 N

| Position 1 | | Position 2 | | Position 3 | |
|------------|-----------|------------|-----------|------------|-----------|
| Node label | U3 | Node label | U3 | Node label | U3 |
| 1288 | -3.52E-01 | 499 | -6.79E-01 | 7 | -8.85E-01 |
| 1289 | -3.41E-01 | 500 | -6.68E-01 | 15 | -8.86E-01 |
| 1290 | -3.29E-01 | 501 | -6.57E-01 | 23 | -8.86E-01 |
| 1292 | -3.30E-01 | 503 | -6.57E-01 | 31 | -8.87E-01 |
| 1293 | -3.41E-01 | 504 | -6.68E-01 | 39 | -8.87E-01 |
| 1294 | -3.52E-01 | 505 | -6.80E-01 | 47 | -8.88E-01 |
| 1296 | -3.52E-01 | 507 | -6.80E-01 | 55 | -8.88E-01 |
| 1297 | -3.41E-01 | 508 | -6.68E-01 | 63 | -8.89E-01 |
| 1298 | -3.30E-01 | 509 | -6.57E-01 | 71 | -8.89E-01 |
| 1300 | -3.30E-01 | 511 | -6.57E-01 | 79 | -8.90E-01 |
| 1301 | -3.41E-01 | 512 | -6.69E-01 | 87 | -8.90E-01 |
| 1302 | -3.53E-01 | 513 | -6.80E-01 | 95 | -8.90E-01 |
| 1304 | -3.53E-01 | 515 | -6.80E-01 | 103 | -8.91E-01 |
| 1305 | -3.42E-01 | 516 | -6.69E-01 | 104 | -9.02E-01 |
| 1306 | -3.30E-01 | 517 | -6.57E-01 | 105 | -9.13E-01 |

| | | | | | |
|------|-----------|-----|-----------|-----|-----------|
| 1308 | -3.31E-01 | 519 | -6.58E-01 | 109 | -8.85E-01 |
| 1309 | -3.42E-01 | 520 | -6.69E-01 | 110 | -8.97E-01 |
| 1310 | -3.53E-01 | 521 | -6.80E-01 | 111 | -9.08E-01 |
| 1312 | -3.53E-01 | 523 | -6.81E-01 | 112 | -8.86E-01 |
| 1313 | -3.42E-01 | 524 | -6.69E-01 | 115 | -8.97E-01 |
| 1314 | -3.31E-01 | 525 | -6.58E-01 | 116 | -9.08E-01 |
| 1316 | -3.31E-01 | 527 | -6.58E-01 | 117 | -8.86E-01 |
| 1317 | -3.42E-01 | 528 | -6.69E-01 | 120 | -8.98E-01 |
| 1318 | -3.54E-01 | 529 | -6.81E-01 | 121 | -9.09E-01 |
| 1320 | -3.54E-01 | 531 | -6.81E-01 | 122 | -8.86E-01 |
| 1321 | -3.43E-01 | 532 | -6.70E-01 | 125 | -8.98E-01 |
| 1322 | -3.31E-01 | 533 | -6.58E-01 | 126 | -9.09E-01 |
| 1324 | -3.31E-01 | 535 | -6.59E-01 | 127 | -8.87E-01 |
| 1325 | -3.43E-01 | 536 | -6.70E-01 | 130 | -8.99E-01 |
| 1326 | -3.54E-01 | 537 | -6.81E-01 | 131 | -9.10E-01 |
| 1328 | -3.54E-01 | 539 | -6.82E-01 | 132 | -8.87E-01 |
| 1329 | -3.43E-01 | 540 | -6.70E-01 | 135 | -8.99E-01 |
| 1330 | -3.32E-01 | 541 | -6.59E-01 | 136 | -9.10E-01 |
| 1332 | -3.32E-01 | 543 | -6.59E-01 | 137 | -8.88E-01 |
| 1333 | -3.43E-01 | 544 | -6.70E-01 | 140 | -9.00E-01 |
| 1334 | -3.55E-01 | 545 | -6.82E-01 | 141 | -9.11E-01 |
| 1336 | -3.55E-01 | 547 | -6.82E-01 | 142 | -8.88E-01 |
| 1337 | -3.44E-01 | 548 | -6.71E-01 | 145 | -9.00E-01 |
| 1338 | -3.32E-01 | 549 | -6.59E-01 | 146 | -9.11E-01 |
| 1340 | -3.32E-01 | 551 | -6.60E-01 | 147 | -8.89E-01 |
| 1341 | -3.44E-01 | 552 | -6.71E-01 | 150 | -9.01E-01 |
| 1342 | -3.55E-01 | 553 | -6.82E-01 | 151 | -9.12E-01 |
| 1344 | -3.55E-01 | 555 | -6.83E-01 | 152 | -8.89E-01 |
| 1345 | -3.44E-01 | 556 | -6.71E-01 | 155 | -9.01E-01 |
| 1346 | -3.33E-01 | 557 | -6.60E-01 | 156 | -9.12E-01 |
| 1348 | -3.33E-01 | 559 | -6.60E-01 | 157 | -8.90E-01 |
| 1349 | -3.44E-01 | 560 | -6.71E-01 | 160 | -9.01E-01 |
| 1350 | -3.56E-01 | 561 | -6.83E-01 | 161 | -9.13E-01 |
| 1352 | -3.56E-01 | 563 | -6.83E-01 | 162 | -8.90E-01 |
| 1353 | -3.45E-01 | 564 | -6.72E-01 | 165 | -9.02E-01 |
| 1354 | -3.33E-01 | 565 | -6.60E-01 | 166 | -9.13E-01 |
| 1356 | -3.33E-01 | 567 | -6.61E-01 | 274 | -8.97E-01 |
| 1357 | -3.45E-01 | 568 | -6.72E-01 | 275 | -9.08E-01 |
| 1358 | -3.56E-01 | 569 | -6.83E-01 | 278 | -8.97E-01 |
| 1360 | -3.56E-01 | 571 | -6.84E-01 | 279 | -9.08E-01 |
| 1361 | -3.45E-01 | 572 | -6.72E-01 | 282 | -8.97E-01 |
| 1362 | -3.34E-01 | 573 | -6.61E-01 | 283 | -9.09E-01 |
| 1364 | -3.34E-01 | 575 | -6.61E-01 | 286 | -8.98E-01 |
| 1365 | -3.45E-01 | 576 | -6.72E-01 | 287 | -9.09E-01 |
| 1366 | -3.57E-01 | 577 | -6.84E-01 | 290 | -8.98E-01 |
| 1368 | -3.57E-01 | 579 | -6.84E-01 | 291 | -9.10E-01 |

| | | | | | |
|------|-----------|-----|-----------|-----|-----------|
| 1369 | -3.46E-01 | 580 | -6.73E-01 | 294 | -8.99E-01 |
| 1370 | -3.34E-01 | 581 | -6.61E-01 | 295 | -9.10E-01 |
| 1372 | -3.34E-01 | 583 | -6.61E-01 | 298 | -8.99E-01 |
| 1373 | -3.46E-01 | 584 | -6.73E-01 | 299 | -9.11E-01 |
| 1374 | -3.57E-01 | 585 | -6.84E-01 | 302 | -9.00E-01 |
| 1376 | -3.57E-01 | 587 | -6.84E-01 | 303 | -9.11E-01 |
| 1377 | -3.46E-01 | 588 | -6.73E-01 | 306 | -9.00E-01 |
| 1378 | -3.35E-01 | 589 | -6.62E-01 | 307 | -9.12E-01 |
| 1380 | -3.35E-01 | 591 | -6.62E-01 | 310 | -9.01E-01 |
| 1381 | -3.46E-01 | 592 | -6.73E-01 | 311 | -9.12E-01 |
| 1382 | -3.58E-01 | 593 | -6.85E-01 | 314 | -9.01E-01 |
| 1384 | -3.58E-01 | 595 | -6.85E-01 | 315 | -9.13E-01 |
| 1385 | -3.46E-01 | 596 | -6.73E-01 | 318 | -9.02E-01 |
| 1386 | -3.35E-01 | 597 | -6.62E-01 | 319 | -9.13E-01 |
| 1388 | -3.35E-01 | 599 | -6.62E-01 | | |
| 1389 | -3.47E-01 | 600 | -6.74E-01 | | |
| 1390 | -3.58E-01 | 601 | -6.85E-01 | | |

AVERAGE -3.44E-01

-6.71E-01

-8.99E-01